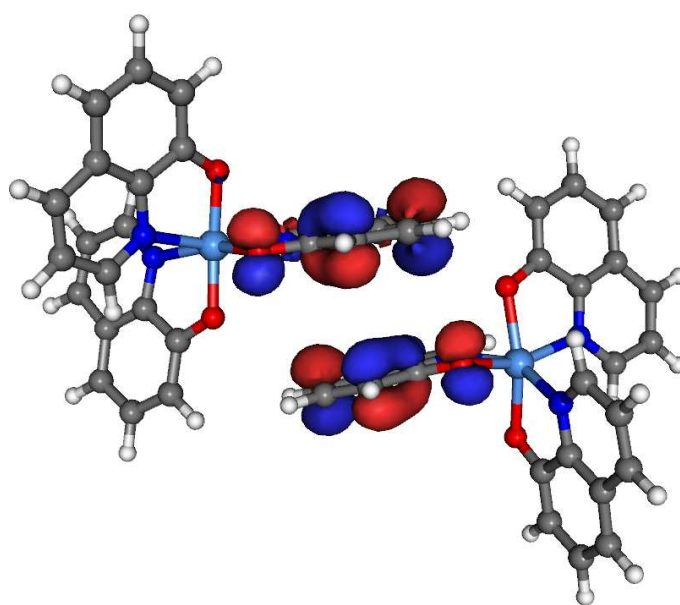


VOTCA-XTP

EXCITON TRANSPORT SIMULATIONS

USER MANUAL



compiled from: 1.4_rc1

September 26, 2016

www.votca.org

Disclaimer

This manual is not complete. The best way to start using the software is to look at provided tutorials. The reference section is generated automatically from the source code, so please make sure that your software and manual versions match.

Citations

Development of this software depends on academic research grants. If you are using the package, please cite the following papers

[1] Microscopic simulations of charge transport in disordered organic semiconductors, Victor Rühle, Alexander Lukyanov, Falk May, Manuel Schrader, Thorsten Vehoff, James Kirkpatrick, Björn Baumeier and Denis Andrienko
J. Chem. Theor. Comp. **7**, 3335, 2011

[2] Versatile Object-oriented Toolkit for Coarse-graining Applications
Victor Rühle, Christoph Junghans, Alexander Lukyanov, Kurt Kremer and Denis Andrienko
J. Chem. Theor. Comp. **5**, 3211, 2009

Development

The core development is currently taking place at the Max Planck Institute for Polymer Research, Mainz, Germany and TU/e Eindhoven.

Copyright

VOTCA-XTP is free software. The entire package is available under the Apache License. For details, check the LICENSE file in the source code. The VOTCA-XTP source code is available on our homepage, www.votca.org.

Contents

1	Introduction	3
2	Theoretical background	5
2.1	Workflow	5
2.2	Material morphology	5
2.3	Conjugated segments and rigid fragments	6
2.4	Neighbor list	8
2.5	Reorganization energy	8
2.5.1	Intramolecular reorganization energy	8
2.5.2	Outersphere reorganization energy	9
2.6	Site energies	10
2.6.1	Externally applied electric field	10
2.6.2	Internal energy	10
2.6.3	Electrostatic interaction energy	11
2.6.4	Induction energy - the Thole model	12
2.7	Transfer integrals	14
2.7.1	Projection of monomer orbitals on dimer orbitals (DIPRO)	14
2.7.2	DFT-based transfer integrals using DIPRO	17
2.7.3	ZINDO-based transfer integrals using MOO	18
2.8	Charge transfer rate	19
2.8.1	Classical charge transfer rate	19
2.8.2	Semi-classical bimolecular rate	19
2.8.3	Semi-classical rate	20
2.9	Master equation	20
2.9.1	Extrapolation to nondispersive mobilities	21
2.10	Stochastic Networks	21
2.10.1	Coarse-grained morphology	22
2.10.2	Charge transport network	25
2.11	Macroscopic observables	29
2.11.1	Charge density	29
2.11.2	Current	30
2.11.3	Mobility and diffusion constant	30
2.11.4	Spatial correlations of energetic disorder	31
3	Input and output files	33
3.1	Atomistic topology	33
3.2	Mapping file	35
3.3	Molecular orbitals	36
3.4	Monomer calculations for DFT transfer integrals	37
3.5	Pair calculations for DFT transfer integrals	39
3.6	DFT transfer integrals	41
3.7	State file	42

4	Reference	45
4.1	Programs	45
4.1.1	xtp_testsuite	45
4.1.2	xtp_update	45
4.1.3	xtp_update_exciton	45
4.1.4	xtp_basisset	45
4.1.5	xtp_map	46
4.1.6	xtp_run	46
4.1.7	xtp_tools	46
4.1.8	xtp_parallel	46
4.1.9	xtp_dump	47
4.1.10	xtp_overlap	47
4.1.11	xtp_kmc_run	47
4.2	Calculators	47
4.2.1	coupling	48
4.2.2	excitonicoupling	48
4.2.3	gencube	49
4.2.4	log2mps	49
4.2.5	molpol	49
4.2.6	orb2isogwa	50
4.2.7	partialcharges	50
4.2.8	pdb2map	50
4.2.9	pdb2top	50
4.2.10	ptopreader	50
4.2.11	qmanalyze	51
4.2.12	eanalyze	51
4.2.13	eimport	51
4.2.14	einternal	51
4.2.15	emultipole	51
4.2.16	eoutersphere	52
4.2.17	ianalyze	53
4.2.18	iimport	53
4.2.19	izindo	53
4.2.20	jobwriter	53
4.2.21	pairedump	53
4.2.22	panalyze	54
4.2.23	profile	54
4.2.24	rates	54
4.2.25	sandbox	54
4.2.26	stateserver	55
4.2.27	tdump	55
4.2.28	vaverage	55
4.2.29	zmultipole	55
4.2.30	edft	56
4.2.31	idft	56
4.2.32	qmmm	56
4.2.33	xqmultipole	57
4.2.34	energy2xml	58
4.2.35	integrals2xml	58
4.2.36	occupations2xml	58
4.2.37	pairs2xml	58
4.2.38	rates2xml	58
4.2.39	segments2xml	59
4.2.40	trajectory2pdb	59

<i>CONTENTS</i>	v
4.3 Common options	59
Bibliography	61

Index

- charge transfer rate, 19
 - bimolecular, 19
 - classical, 19
 - semiclassical, 20
- conjugated segment, 6
- current, 30
 - local, 30
- diabatic states, 14
- distributed multipoles, 11
- electronic coupling, 14
 - DFT, 17
 - ZINDO, 18
- hopping site, 6
- kinetic Monte Carlo, 20
- mobility, 30
- neighbor list, 8
- Pekar factor, 10
- reorganization energy, 8
 - intramolecular, 8
 - outersphere, 9
- rigid fragment, 7
- site energy, 10
 - distributed multipoles, 11
 - external field, 10
 - internal, 10
 - polarization, 12
 - spatial correlation, 31
- Thole model, 12
- transfer integral, *see* electronic coupling

Chapter 1

Introduction

sec:introduction

Charge carrier dynamics in an organic semiconductor can often be described in terms of charge hopping between localized states. The hopping rates depend on **electronic coupling elements**, **reorganization energies**, and **site energies**, which vary as a function of position and orientation of the molecules. The purpose of the VOTCA-XTP package [1] is to simplify the workflow for charge transport simulations, provide a uniform error-control for the methods, flexible platform for their development, and eventually allow *in silico* prescreening of organic semiconductors for specific applications.

The toolkit is implemented using modular concepts introduced earlier in the Versatile Object-oriented Toolkit for Coarse-graining Applications (VOTCA) [2]. It contains different **programs**, which execute specific tasks implemented in **calculators** representing an individual step in the workflow. Figure 1.1 summarizes a typical chain of commands to perform a charge transport simulation: First, the VOTCA code structures are adapted to reading atomistic trajectories, mapping them onto conjugated segments and rigid fragments, and substituting (if needed) rigid fragments with the optimized copies (`xtp_map`). The programs `xtp_run` and `xtp_parallel` (for heavy-duty tasks) are then used to calculate all bimolecular charge hopping rates (via precalculation of all required ingredients). **Site energies (or energetic disorder)** can be determined as a combination of internal (ionization potentials/electron affinities of single molecules) as well as electrostatic and polarization contributions within the molecular environment. The calculation of **electronic coupling elements** between conjugated segments from the corresponding molecular orbitals can be performed using a **dimer-projection** technique based on **density-functional** theory (DFT). This requires explicit calculations using quantum-chemistry software for which we provide interfaces to `Gaussian`, `Turbomole`, and `NWChem`. Alternatively, the **molecular orbital overlap** module calculates electronic coupling elements relying on the semi-empirical INDO Hamiltonian and molecular orbitals in the format provided by the `Gaussian` package.

The **kinetic Monte Carlo** module reads in the neighbor list, site coordinates, and hopping rates and performs charge dynamics simulations using either periodic boundary conditions or charge sources and sinks.

The toolkit is written as a combination of modular C++ code and scripts. The data transfer between programs is implemented via a state file (sql database), which is also used to restart simulations. Analysis functions and most of the calculation routines are encapsulated by using the observer pattern [3] which allows the implementation of new functions as individual modules.

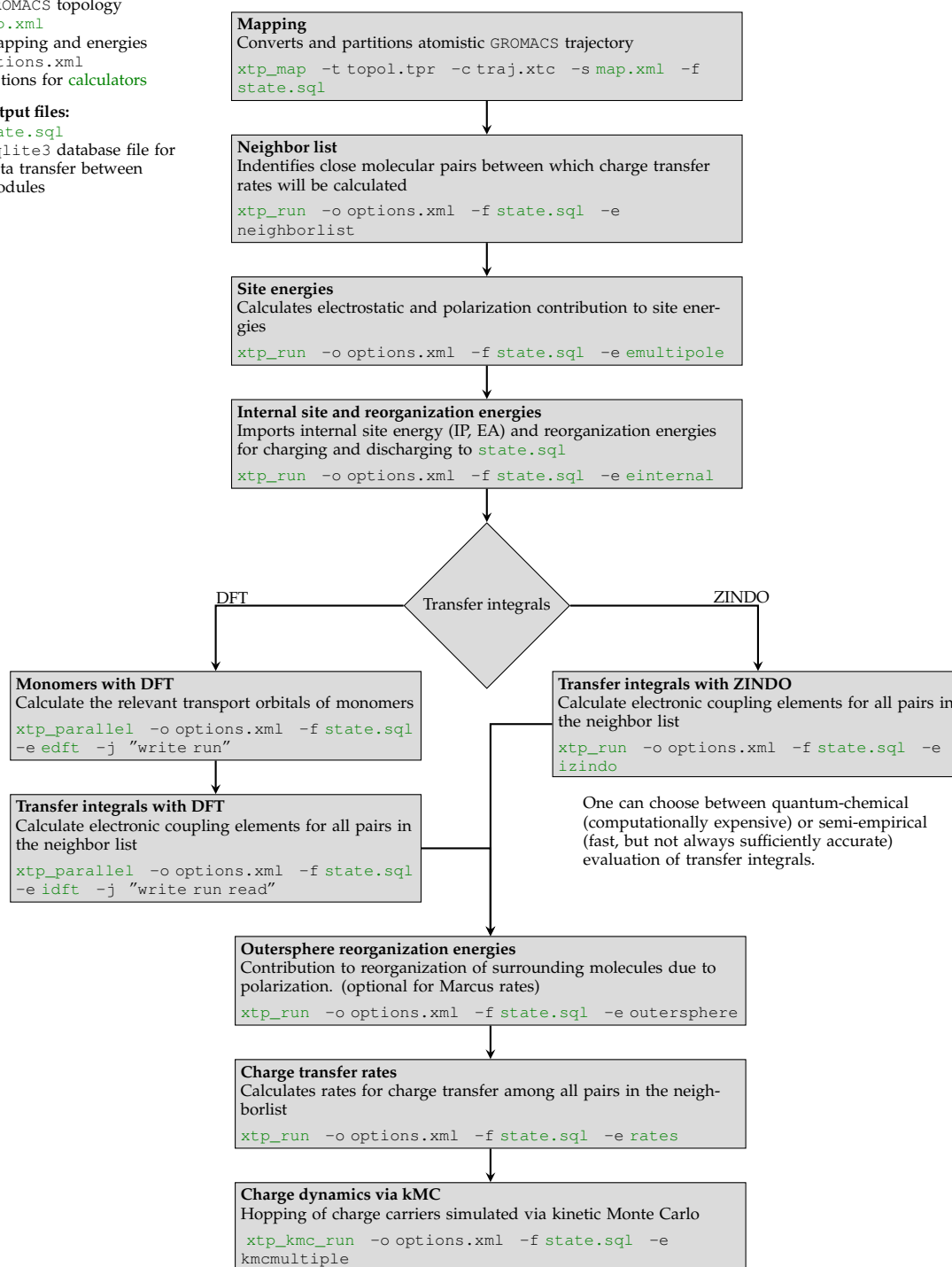
In the following chapter 2, we summarize the **theoretical background** of the workflow of charge transport simulations and in particular its individual steps. Chapter 3 describes the structure and content of input and output files, while a full reference of **programs** and **calculators** is available in chapter 4. For a hands-on tutorial, the reader is referred to the VOTCA-XTP project page at <http://code.google.com/p/votca-xtp/>.

Input files:

conf.gro
GROMACS trajectory
topol.tpr
GROMACS topology
map.xml
mapping and energies
options.xml
options for calculators

Output files:

state.sql
sqlite3 database file for
data transfer between
modules



Get list of available calculators: `xtp_run/xtp_parallel/xtp_kmc_run -l`

Get help and list of options for a calculator: `xtp_run/xtp_parallel/xtp_kmc_run -d neighborlist`

Figure 1.1: A practical workflow of charge transport simulations using VOTCA-XTP. The **theoretical background** of the individual steps is given in chapter 2. Chapter 3 describes the content of input and output files, while a full reference of **programs** and **calculators** is available in chapter 4. fig:summary

Chapter 2

Theoretical background

2.1 Workflow

A typical workflow of charge transport simulations is depicted in figure 2.1. The first step is the simulation of an atomistic morphology, which is then partitioned on hopping sites. The coordinates of the hopping sites are used to construct a list of pairs of molecules, or neighbor list.

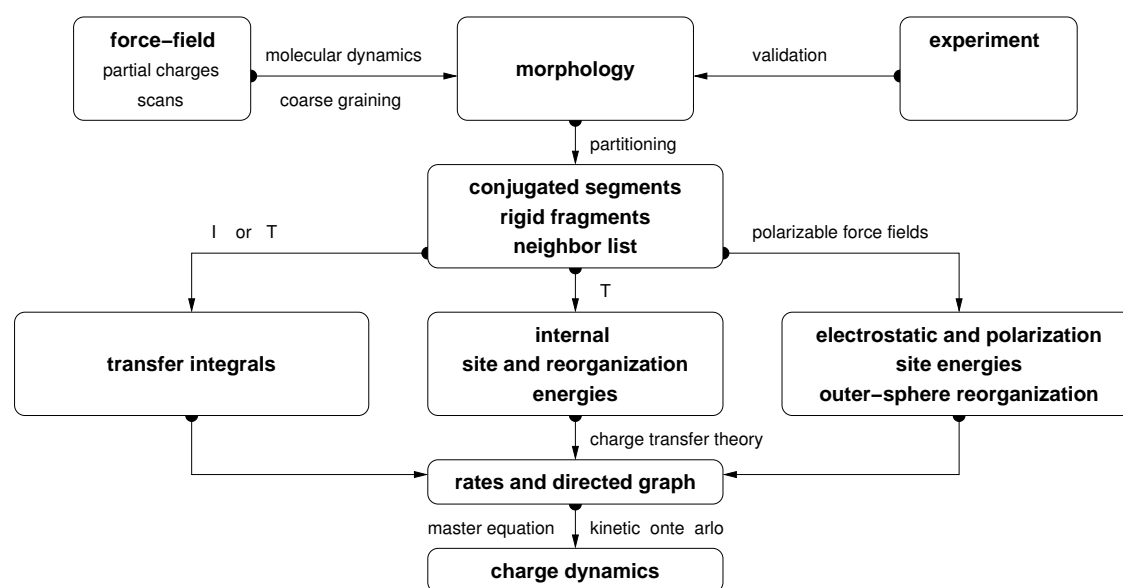


Figure 2.1: Workflow for microscopic simulations of charge transport.

For each pair an electronic coupling element, a reorganization energy, a driving force, and eventually the hopping rate are evaluated. The neighbor list and hopping rates define a directed graph. The corresponding master equation is solved using the kinetic Monte Carlo method, which allows to explicitly monitor the charge dynamics in the system as well as to calculate time or ensemble averages of occupation probabilities, charge fluxes, correlation functions, and field-dependent mobilities.

2.2 Material morphology

There is no generic recipe on how to predict a large-scale atomistically-resolved morphology of an organic semiconductor. The required methods are system-specific: for ultra-pure crystals, for

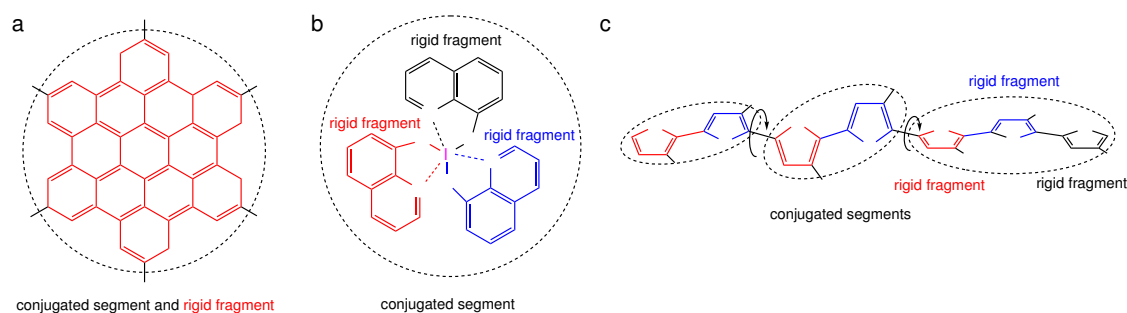


Figure 2.2: The concept of conjugated segments and rigid fragments. Dashed lines indicate conjugated segments while colors denote rigid fragments. (a) Hexabenzocoronene: the π -conjugated system is both a rigid fragment and a conjugated segment. (b) Alq_3 : the Al atom and each ligand are rigid fragments while the whole molecule is a conjugated segment. (c) Polythiophene: each repeat unit is a rigid fragment. A conjugated segment consists of one or more rigid fragments. One molecule can have several conjugated segments.

fig:segment

54 example, density-functional methods can be used provided the crystal structure is known from
 55 experiment. For partially disordered organic semiconductors, however, system sizes much larger
 56 than a unit cell are required. Classical molecular dynamics or Monte Carlo techniques are then
 57 the methods of choice.

58 In molecular dynamics, atoms are represented by point masses which interact via empirical po-
 59 tentials prescribed by a force-field. Force-fields are parametrized for a limited set of compounds
 60 and their refinement is often required for new molecules. In particular, special attention shall
 61 be paid to torsion potentials between successive repeat units of conjugated polymers or between
 62 functional groups and the π -conjugated system. First-principles methods can be used to charac-
 63 terize the missing terms of the potential energy function.

64 Self-assembling materials, such as soluble oligomers, discotic liquid crystals, block copolymers,
 65 partially crystalline polymers, etc., are the most complicated to study. The morphology of such
 66 systems often has several characteristic length scales and can be kinetically arrested in a thermo-
 67 dynamically non-equilibrium state. For such systems, the time- and length-scales of atomistic
 68 simulations might be insufficient to equilibrate or sample desired morphologies. In this case,
 69 systematic coarse-graining can be used to enhance sampling [2]. Note that the coarse-grained
 70 representation must reflect the structure of the atomistic system and allow for back-mapping to
 71 the atomistic resolution.

72 Here we assume that the morphology is already known, that is we know how the topology and
 73 the coordinates of all atoms in the systems at a given time. VOTCA-XTP can read standard
 74 GROMACS topology files. Custom definitions of **atomistic topology** via XML files are also possible.
 75 Since the description of the atomistic topology is the first step in the charge transport simulations,
 76 it is important to follow simple conventions on how the system is partitioned on molecules,
 77 residues, and how atoms are named in the topology. Required input files are described in section
 78 **atomistic topology**.

79 2.3 Conjugated segments and rigid fragments

sec:segments

80 With the morphology at hand, the next step is partitioning the system on hopping sites, or con-
 81 jugated segments, and calculating charge transfer rates between them. Physically intuitive argu-
 82 ments can be used for the partitioning, which reflects the localization of the wave function of
 83 a charge. For most organic semiconductors, the molecular architecture includes relatively rigid,
 84 planar π -conjugated systems, which we will refer to as rigid fragments. A conjugated segment
 85 can contain one or more of such rigid fragments, which are linked by bonded degrees of freedom.

86 The dynamics of these degrees of freedom evolves on timescales much slower than the frequency
 87 of the internal promoting mode. In some cases, e.g. glasses, it can be ‘frozen’ due to non-bonded
 88 interactions with the surrounding molecules.

89 To illustrate the concept of conjugated segments and rigid fragments, three representative molec-
 90 ular architectures are shown in figure 2.2. The first one is a typical discotic liquid crystal, hex-
 91 abenzocoronene. It consists of a conjugated core to which side chains are attached to aid self-
 92 assembly and solution processing. In this case the orbitals localized on side chains do not partic-
 93 ipate in charge transport and the conjugated π -system is both, a rigid fragment and a conjugated
 94 segment. In Alq_3 , a metal-coordinated compound, a charge carrier is delocalized over all three
 95 ligands. Hence, the whole molecule is one conjugated segment. Individual ligands are relatively
 96 rigid, while energies of the order of $k_B T$ are sufficient to reorient them with respect to each other.
 97 Thus the Al atom and the three ligands are rigid fragments. In the case of a conjugated polymer,
 98 one molecule can consist of several conjugated segments, while each backbone repeat unit is a
 99 rigid fragment. Since the conjugation along the backbone can be broken due to large out-of-plane
 100 twists between two repeat units, an empirical criterion, based on the dihedral angle, can be used
 101 to partition the backbone on conjugated segments [4]. However, such intuitive partitioning is, to
 102 some extent, arbitrary and shall be validated by other methods [5–7].

103 After partitioning, an additional step is often required to remove bond length fluctuations intro-
 104 duced by molecular dynamics simulations, since they are already integrated out in the deriva-
 105 tion of the rate expression. This is achieved by substituting respective molecular fragments with
 106 rigid, planar π -systems optimized using first-principles methods. Centers of mass and gyration
 107 tensors are used to align rigid fragments, though a custom definition of local axes is also possible.
 108 Such a procedure also minimizes discrepancies between the force-field and first-principles-based
 109 ground state geometries of conjugated segments, which might be important for calculations of
 110 electronic couplings, reorganization energies, and intramolecular driving forces.

111 To partition the system on hopping sites and substitute rigid fragments with the corresponding
 112 ground-state geometries `xtp_map` program is used:

Mapping the GROMACS trajectory

```
| xtp_map -t topol.tpr -c traj.xtc -s map.xml -f state.sql
```

113
 114 It reads in the GROMACS topology (`topol.tpr`) and trajectory (`traj.xtc`) files, definitions of
 115 conjugated segments and rigid fragments (`map.xml`) and outputs coordinates of conjugated seg-
 116 ments (hopping sites) and rigid fragments (as provided in the MD trajectory and after rigidi-
 117 fication) to the state file (`state.sql`). In order to do this, a mapping file `map.xml` has to be
 118 provided, which specifies the corresponding atoms in the different representations. After this
 119 step, all information (frame number, dimensions of the simulation box, etc) are stored in the state
 120 file and only this file is used for further calculations.

Be careful!

121 | VOTCA-XTP requires a wrapped trajectory for mapping the segments and fragments, so all
 molecules should be whole in the frame.

122 In order to visually check the mapping one can use either the `tdump` calculator or the programm
 123 `xtp_dump` with the calculator `trajectory2pdb`.

Writing a mapped trajectory with `xtp_dump`

```
| xtp_dump -f state.sql -e trajectory2pdb
```

124
 125 It reads in the state file created by `xtp_map` and outputs two trajectory files corresponding to
 126 the original and rigidified atom coordinates. To check the mapping, it is useful to superimpose
 127 the three outputs (original atomistic, atomistic stored in the state file, and rigidified according to
 128 ground state geometries), e.g., with VMD.

Writing a mapped trajectory with `tdump`

```
| xtp_run -f state.sql -o options.xml -e tdump
```

129

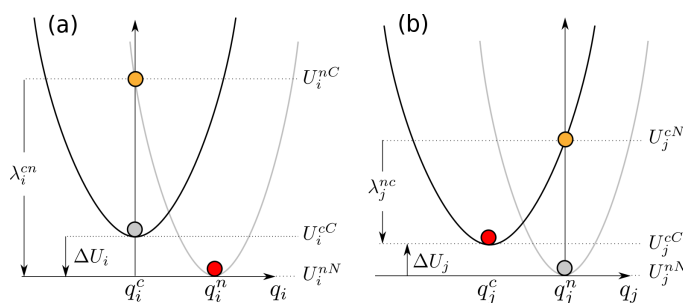


Figure 2.3: Potential energy surfaces of (a) donor and (b) acceptor in charged and neutral states. After the change of the charge state both molecules relax their nuclear coordinates. If all vibrational modes are treated classically, the total internal reorganization energy and the internal energy difference of the electron transfer reaction are $\lambda_{ij}^{\text{int}} = \lambda_i^{cn} + \lambda_j^{nc}$ and $\Delta E_{ij}^{\text{int}} = \Delta U_i - \Delta U_j$, respectively.

fig.parabolas

130 It also reads in the state file but appends the coordinates to a pdb. file. So make sure to delete old
 131 QM.pdb and MD.pdb if you want to create a new imagef

132 2.4 Neighbor list

sec.neighborlist

133 A list of neighboring conjugated segments, or neighbor list, contains all pairs of conjugated seg-
 134 ments for which **coupling elements**, **reorganization energies**, **site energy differences**, and **rates**
 135 are evaluated.

136 Two segments are added to this list if the distance between centers of mass of any of their rigid
 137 fragments is below a certain cutoff. This allows neighbors to be selected on a criterion of min-
 138 imum distance of approach rather than center of mass distance, which is useful for molecules
 139 with anisotropic shapes.

140 The neighbor list can be generated from the atomistic trajectory by using the `neighborlist`
 141 `calculator`. This calculator requires a cutoff, which can be specified in the `options.xml` file. The
 142 list is saved to the `state.sql` file:

Generating a neighbor list

```
| xtp_run -o options.xml -f state.sql -e neighborlist
```

143

144 2.5 Reorganization energy

sec.reorganization

145 The reorganization energy λ_{ij} takes into account the change in nuclear (and dielectric) degrees of
 146 freedom as the charge moves from donor i to acceptor j . It has two contributions: intramolecular,
 147 $\lambda_{ij}^{\text{int}}$, which is due to reorganization of nuclear coordinates of the two molecules forming the
 148 charge transfer complex, and intermolecular (outersphere), $\lambda_{ij}^{\text{out}}$, which is due to the relaxation of
 149 the nuclear coordinates of the environment. In what follows we discuss how these contributions
 150 can be calculated.

151 2.5.1 Intramolecular reorganization energy

sec.intramolecular

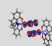
152 If intramolecular vibrational modes of the two molecules are treated classically, the rearrange-
 153 ment of their nuclear coordinates after charge transfer results in the dissipation of the internal
 154 reorganization energy, $\lambda_{ij}^{\text{int}}$. It can be computed from four points on the potential energy surfaces
 155 (PES) of both molecules in neutral and charged states, as indicated in figure 2.3.

156 Adding the contributions due to discharging of molecule i and charging of molecule j yields [8]

$$\lambda_{ij}^{\text{int}} = \lambda_i^{\text{cn}} + \lambda_j^{\text{nc}} = U_i^{\text{nC}} - U_i^{\text{nN}} + U_j^{\text{cN}} - U_j^{\text{cC}}. \quad (2.1) \quad \text{equ:lambda_das}$$

157 Here U_i^{nC} is the internal energy of the neutral molecule i in the geometry of its charged state
 158 (small n denotes the state and capital C the geometry). Similarly, U_j^{cN} is the energy of the charged
 159 molecule j in the geometry of its neutral state. Note that the PES of the donor and acceptor are
 160 not identical for chemically different compounds or for conformers of the same molecule. In this
 161 case $\lambda_i^{\text{cn}} \neq \lambda_j^{\text{cn}}$ and $\lambda_i^{\text{nc}} \neq \lambda_j^{\text{nc}}$. Thus $\lambda_{ij}^{\text{int}}$ is a property of the charge transfer complex, and not of
 162 a single molecule.

163 Intramolecular reorganization energies for discharging (λ^{cn}) and charging (λ^{nc}) of a molecule
 164 need to be determined using quantum-chemistry and given in `map.xml`. The values are written
 165 to the `state.sql` using the calculator `einternal` (see also internal energy):

```
166  Intramolecular reorganization energies
| xtp_run -o options.xml -f state.sql -e einternal
```

167 2.5.2 Outersphere reorganization energy

sec:outersphere

168 During the charge transfer reaction, also the molecules outside the charge transfer complex reori-
 169 ent and polarize in order to adjust for changes in electric potential, resulting in the outersphere
 170 contribution to the reorganization energy. $\lambda_{ij}^{\text{out}}$ is particularly important if charge transfer occurs
 171 in a polarizable environment. Assuming that charge transfer is much slower than electronic po-
 172 larization but much faster than nuclear rearrangement of the environment, $\lambda_{ij}^{\text{out}}$ can be calculated
 173 from the electric displacement fields created by the charge transfer complex [9]

$$\lambda_{ij}^{\text{out}} = \frac{c_p}{2\epsilon_0} \int_{V^{\text{out}}} dV \left[\vec{D}_I(\vec{r}) - \vec{D}_F(\vec{r}) \right]^2, \quad (2.2) \quad \text{equ:lambda_outer1}$$

174 where ϵ_0 is the the permittivity of free space, $\vec{D}_{I,F}(\vec{r})$ are the electric displacement fields created
 175 by the charge transfer complex in the initial (charge on molecule i) and final (charge transferred
 176 to molecule j) states, V^{out} is the volume outside the complex, and $c_p = \frac{1}{\epsilon_{\text{opt}}} - \frac{1}{\epsilon_s}$ is the Pekar factor,
 177 which is determined by the low (ϵ_s) and high (ϵ_{opt}) frequency dielectric permittivities.

178 Eq. (2.2) can be simplified by assuming spherically symmetric charge distributions on molecules
 179 i and j with total charge e . Integration over the volume V^{out} outside of the two spheres of radii R_i
 180 and R_j centered on molecules i and j leads to the classical Marcus expression for the outersphere
 181 reorganization energy

$$\lambda_{ij}^{\text{out}} = \frac{c_p e^2}{4\pi\epsilon_0} \left(\frac{1}{2R_i} + \frac{1}{2R_j} - \frac{1}{r_{ij}} \right), \quad (2.3) \quad \text{equ:lambda_outer2}$$

182 where r_{ij} is the molecular separation. While eq. (2.3) captures the main physics, e.g. predicts
 183 smaller outer-sphere reorganization energies (higher rates) for molecules at smaller separations,
 184 it often cannot provide quantitative estimates, since charge distributions are rarely spherically
 185 symmetric.

186 Alternatively, the displacement fields can be constructed using the atomic partial charges. The
 187 difference of the displacement fields at the position of an atom b_k outside the charge transfer
 188 complex (molecule $k \neq i, j$) can be expressed as

$$\vec{D}_I(\vec{r}_{b_k}) - \vec{D}_F(\vec{r}_{b_k}) = \sum_{a_i} \frac{q_{a_i}^c - q_{a_i}^n}{4\pi} \frac{(\vec{r}_{b_k} - \vec{r}_{a_i})}{|\vec{r}_{b_k} - \vec{r}_{a_i}|^3} + \sum_{a_j} \frac{q_{a_j}^n - q_{a_j}^c}{4\pi} \frac{(\vec{r}_{b_k} - \vec{r}_{a_j})}{|\vec{r}_{b_k} - \vec{r}_{a_j}|^3}, \quad (2.4)$$

189 where $q_{a_i}^n$ ($q_{a_i}^c$) is the partial charge of atom a of the neutral (charged) molecule i in vacuum. The
 190 partial charges of neutral and charged molecules are obtained by fitting their values to reproduce

191 the electrostatic potential of a single molecule (charged or neutral) in vacuum. Assuming a uni-
 192 form density of atoms, the integration in eq. (2.2) can be rewritten as a density-weighted sum
 193 over all atoms excluding those of the charge transfer complex.

194 The remaining unknown needed to calculate $\lambda_{ij}^{\text{out}}$ is the Pekar factor, c_p . In polar solvents $\epsilon_s \gg$
 195 $\epsilon_{\text{opt}} \sim 1$ and c_p is of the order of 1. In most organic semiconductors, however, molecular orien-
 196 tations are fixed and therefore the low frequency dielectric permittivity is of the same order of
 197 magnitude as ϵ_{opt} . Hence, c_p is small and its value is very sensitive to differences in the permit-
 198 tivities.

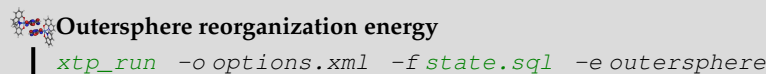
199 Outersphere reorganization energies for all pairs of molecules in the `neighbor list` can be com-
 200 puted from the atomistic trajectory by using the `eoutersphere calculator`.

201 Two methods can be used to compute $\lambda_{ij}^{\text{out}}$. The first method uses the atomistic partial charges of
 202 neutral and charged molecules from files specified in `map.xml` and eq. (2.2). The Pekar factor c_p
 203 and a cutoff radius based on molecular centers of mass have to be specified in the `options.xml`
 204 file.

205 If this method is computationally prohibitive, $\lambda_{ij}^{\text{out}}$ can be computed using eq. (2.3), which as-
 206 sumes spherical charge distributions on the molecules. In this case the radii of these spheres are
 207 specified in `segments.xml`, while the Pekar factor c_p is given in the `options.xml` file and no
 208 cutoff radius is needed.

209 The outer sphere reorganization energies are saved to the `state.sql` file:

```

  210 
  | xtp_run -o options.xml -f state.sql -e outersphere
  
```

211 2.6 Site energies

sec:site_energies

212 A charge transfer reaction between molecules i and j is driven by the site energy difference,
 213 $\Delta E_{ij} = E_i - E_j$. Since the transfer rate, ω_{ij} , depends exponentially on ΔE_{ij} (see eq. (2.31)) it is
 214 important to compute its distribution as accurately as possible. The total site energy difference
 215 has contributions due to `externally applied electric field`, electrostatic interactions, polarization
 216 effects, and `internal energy` differences. In what follows we discuss how to estimate these contri-
 217 butions by making use of first-principles calculations and polarizable force-fields.

218 2.6.1 Externally applied electric field

sec:ext_field

219 The contribution to the total site energy difference due to an external electric field \vec{F} is given by
 220 $\Delta E_{ij}^{\text{ext}} = q\vec{F} \cdot \vec{r}_{ij}$, where $q = \pm e$ is the charge and $\vec{r}_{ij} = \vec{r}_i - \vec{r}_j$ is a vector connecting molecules
 221 i and j . For typical distances between small molecules, which are of the order of 1 nm, and
 222 moderate fields of $F < 10^8$ V/m this term is always smaller than 0.1 eV.

223 2.6.2 Internal energy

sec:internal_energy

224 The contribution to the site energy difference due to different internal energies (see figure 2.3)
 225 can be written as

$$\Delta E_{ij}^{\text{int}} = \Delta U_i - \Delta U_j = (U_i^{cC} - U_i^{nN}) - (U_j^{cC} - U_j^{nN}), \quad (2.5) \quad \text{equ:conformational}$$

226 where $U_i^{cC(nN)}$ is the total energy of molecule i in the charged (neutral) state and geometry. ΔU_i
 227 corresponds to the adiabatic ionization potential (or electron affinity) of molecule i , as shown
 228 in figure 2.3. For one-component systems and negligible conformational changes $\Delta E_{ij}^{\text{int}} = 0$,
 229 while it is significant for donor-acceptor systems.

230 Internal energies determined using quantum-chemistry need to be specified in `map.xml`. The
 231 values are written to the `state.sql` using the calculator `einternal` (see also `intramolecular`
 232 `reorganization energy`):



Internal energies

```
| xtp_run -o options.xml -f state.sql -e einternal
```

233

234 2.6.3 Electrostatic interaction energy

sec.distributed_multipoles

We represent the molecular charge density by choosing multiple expansion sites (“polar sites”) per molecule in such a way as to accurately reproduce the molecular electrostatic potential (ESP), with a set of suitably chosen multipole moments $\{Q_{lk}^a\}$ (in spherical-tensor notation) allocated to each site. The expression for the electrostatic interaction energy between two molecules A and B in the multi-point expansion includes an implicit sum over expansion sites $a \in A$ and $b \in B$,

$$U_{AB} = \sum_{a \in A} \sum_{b \in B} \hat{Q}_{l_1 k_1}^a T_{l_1 k_1 l_2 k_2}^{a,b} \hat{Q}_{l_2 k_2}^b \equiv \hat{Q}_{l_1 k_1}^a T_{l_1 k_1 l_2 k_2}^{a,b} \hat{Q}_{l_2 k_2}^b, \quad (2.6)$$

equ.mol_distributed_U

235 where we have used the Einstein sum convention for the site indices a and b on the right-hand
 236 side of the equation, in addition to the sum convention that is in place for the multipole-moment
 237 components $t \equiv l_1 k_1$ and $u \equiv l_2 k_2$. The $T_{l_1 k_1 l_2 k_2}^{a,b}$ are tensors that mediate the interaction between
 238 a multipole component $l_1 k_1$ on site a with the moment $l_2 k_2$ on site b . If we include the molecular
 239 environment into a perturbative term W to enter in the single-molecule Hamiltonian, the above
 240 expression is exactly the first-order correction to the energy where the quantum-mechanical detail
 241 has been absorbed in classical multipole moments.

242 There are a number of strategies how to arrive at such a collection of *distributed multipoles*. They can
 243 be classified according to whether the multipoles are derived (a) from the electrostatic potential
 244 generated by the SCF charge density or (b) from a decomposition of the wavefunction itself. Here,
 245 we will only draft two of those approaches, CHELPG [10] from category (a) and DMA [11] from
 246 category (b).

The CHELPG (Charges from Electrostatic Potentials, Grid-based) method relies on performing a least-squares fit of atom-placed charges to reproduce the electrostatic potential as evaluated from the SCF density on a regularly spaced grid [10]. The fitted charges result from minimizing the Lagrangian function [12]

$$z(\{q_i\}) = \sum_{k=1}^M \left(\phi(\vec{r}_k) - \sum_{i=1}^N \frac{1}{4\pi\epsilon_0} \frac{q_i}{|\vec{r}_i - \vec{r}_k|} \right) + \lambda \left(q_{\text{mol}} - \sum_{i=1}^N q_i \right), \quad (2.7)$$

247 with M grid points, N atomic sites, the set of atomic partial charges $\{q_i\}$ and the SCF potential ϕ .
 248 The Lagrange multiplier λ constrains the sum of the fitted charges to the molecular charge q_{mol} .
 249 The main difference from other fitting schemes [13] is the algorithm that selects the positions
 250 at which the potential is evaluated (we note that the choice of grid points can have substantial
 251 effects especially for bulky molecules). Clearly, the CHELPG method can be (and has been)
 252 extended to include higher atomic multipoles. It should be noted, however, how already the in-
 253 clusion of atomic dipoles hardly improves the parametrization, and can in fact be harmful to its
 254 conformational stability.

The Distributed-Multipole-Analysis (DMA) approach [11, 14], developed by A. Stone, operates directly on the quantum-mechanical density matrix, expanded in terms of atom- and bond-centered Gaussian functions $\chi_\alpha = R_{LK}(\vec{x} - \vec{s}_\alpha) \exp[-\zeta(\vec{x} - \vec{s}_\alpha)^2]$,

$$\rho(\vec{x}) = \sum_{\alpha,\beta} \rho_{\alpha\beta} \chi_\alpha(\vec{x} - \vec{s}_\alpha) \chi_\beta(\vec{x} - \vec{s}_\beta). \quad (2.8)$$

The aim is to compute multipole moments according in a distributed fashion: If we use that the overlap product $\chi_\alpha \chi_\beta$ of two Gaussian basis functions yields itself a Gaussian centered at $\vec{P} = (\zeta_\alpha \vec{s}_\alpha + \zeta_\beta \vec{s}_\beta) / (\zeta_\alpha + \zeta_\beta)$, it is possible to proceed in two steps: First, we compute the multipole

moments associated with a specific summand in the density matrix, referred to the overlap center \vec{P} :

$$Q_{LK}[\vec{P}] = - \int R_{LK}(\vec{x} - \vec{P}) \rho_{\alpha\beta} \chi_{\alpha} \chi_{\beta} d^3x. \quad (2.9)$$

Second, we transfer the resulting $Q_{lk}[\vec{P}]$ to the position \vec{S} of a polar site according to the rule [11]

$$Q_{nm}[\vec{S}] = \sum_{l=0}^L \sum_{k=-l}^l \left[\binom{n+m}{l+k} \binom{n-m}{l-k} \right]^{1/2} R_{n-l, m-k}(\vec{S} - \vec{P}) \cdot Q_{lk}[\vec{P}]. \quad (2.10)$$

255 Note how this requires a rule for the choice of the expansion site to which the multipole moment
 256 should be transferred. In the near past [14], the nearest-site algorithm, which allocates the mul-
 257 tipole moments to the site closest to the overlap center, was replaced for diffuse functions by an
 258 algorithm based on a sxtpth weighting function in conjunction with grid-based integration meth-
 259 ods in order to decrease the basis-set dependence of the resulting set of distributed multipoles.
 260 One important advantage of the DMA approach over fitting algorithms such as CHELPG or
 261 Merz-Kollman (MK) is that higher-order moments can also be derived without too large an am-
 262 biguity.

263 The ‘mps’ file format used by VOTCA for the definition of distributed multipoles (as well as
 264 point polarizabilities, see subsequent section) is based on the GDMA punch format of A. Stone’s
 265 GDMA program [14] (the punch output file can be immediately plugged into VOTCA without
 266 any conversions to be applied). Furthermore the log-file of different QM packages (currently
 267 Gaussian, Turbomole and NWChem) may be fed into the `log2mps` tool, which will subse-
 268 quently generate the appropriate mps-file.

```

 Read in ESP charges from a QM log file
| xtp_tools -o options.xml -e log2mps
  
```

269 2.6.4 Induction energy - the Thole model

270 If we in addition to the permanent set of multipole moments $\{Q_t^a\}$ allow for induced moments
 { ΔQ_t^a } and penalize their generation with a bilinear form (giving rise to a strictly positive con-
 tribution to the energy),

$$U_{\text{int}} = \frac{1}{2} \sum_A \Delta Q_t^a \eta_{tt'}^{aa'} \Delta Q_{t'}^{a'}, \quad (2.11)$$

it can be shown that the induction contribution to the site energy evaluates to an expression
 where all interactions between induced moments have cancelled out, and interactions between
 permanent and induced moments are scaled down by 1/2 [15]:

$$U_{pu} = \frac{1}{2} \sum_A \sum_{B>A} [\Delta Q_t^a T_{tu}^{ab} Q_u^b + \Delta Q_t^b T_{tu}^{ab} Q_u^a]. \quad (2.12) \quad \text{equ:u_pu}$$

This term can be viewed as the second-order (induction) correction to the molecular interaction
 energy. The sets of $\{Q_t^a\}$ are solved for self-consistently via

$$\Delta Q_t^a = - \sum_{B \neq A} \alpha_{tt'}^{aa'} T_{t'u}^{a'b} (Q_u^b + \Delta Q_u^b), \quad (2.13) \quad \text{equ:self_consistent_dQ}$$

271 where the polarizability tensors $\alpha_{tt'}^{aa'}$ are given by the inverse of $\eta_{tt'}^{aa'}$.

272 With eqs. 2.13 and 2.12 we have at hand expressions that allow us to compute the induction en-
 273 ergy contribution to site energies in an iterative manner based on a set of molecular distributed

274 multipoles $\{Q_t^a\}$ and polarizabilities $\{\alpha_{tt'}^{aa'}\}$. We have drafted in the previous section how to ob-
 275 tain the former from a wavefunction decomposition or fitting scheme (GDMA, CHELPG). The
 276 $\{\alpha_{tt'}^{aa'}\}$ can be derived formally (or rather: read off) from a perturbative expansion of the molec-
 277 ular interaction. In this work we make use of the Thole model [16, 17] as a semi-empirical ap-
 278 proach to obtain the sought-after point polarizabilities in the local dipole approximation, that is,
 279 $[\alpha_{tt'}^{aa'}] = \alpha_{tt'}^{aa'} \delta_{t\beta} \delta_{t'\beta} \delta_{aa'}$, where $\beta \in \{x, y, z\}$ references the dipole-moment component.
 280 The Thole model is based on a modified dipole-dipole interaction, which can be reformulated in
 281 terms of the interaction of smeared charge densities. This has been shown to be necessary due
 282 to the divergent head-to-tail dipole-dipole interaction that otherwise results at small intersepara-
 283 tions on the Å scale [16–18]. Smearing out the charge distribution mimics the nature of the QM
 284 wavefunction, which effectively guards against this unphysical polarization catastrophe. Since
 285 the point dipoles however only react individually to the external field, any correlation effects as
 286 were still accounted for in the $\{\alpha_{tt'}^{aa'}\}$ are lost, except perhaps those correlations that are due to
 287 the mere classical field interaction.

The smearing of the nuclei-centered multipole moments is obtained via a fractional charge den-
 sity $\rho_f(\vec{u})$ which should be normalized to unity and fall off rapidly as of a certain radius $\vec{u} = \vec{u}(\vec{R})$.
 The latter is related to the physical distance vector \vec{R} connecting two interacting sites via a linear
 scaling factor that takes into account the magnitude of the isotropic site polarizabilities α^a . This
 isotropic fractional charge density gives rise to a modified potential

$$\phi(u) = -\frac{1}{4\pi\epsilon_0} \int_0^u 4\pi u' \rho(u') du' \quad (2.14) \quad \text{equ:mod_potential}$$

We can relate the multipole interaction tensor $T_{ij\dots}$ (this time in Cartesian coordinates) to the
 fractional charge density in two steps: First, we rewrite the tensor in terms of the scaled distance
 vector \vec{u} ,

$$T_{ij\dots}(\vec{R}) = f(\alpha^a \alpha^b) t_{ij\dots}(\vec{u}(\vec{R}, \alpha^a \alpha^b)), \quad (2.15)$$

where the specific form of $f(\alpha^a \alpha^b)$ results from the choice of $u(\vec{R}, \alpha^a \alpha^b)$. Second, we demand
 that the smeared interaction tensor $t_{ij\dots}$ is given as usual by the appropriate derivative of the
 potential in eq. 2.14,

$$t_{ij\dots}(\vec{u}) = -\partial_{u_i} \partial_{u_j} \dots \phi(\vec{u}). \quad (2.16)$$

288 It turns out that for a suitable choice of $\rho_f(\vec{u})$, the modified interaction tensors can be rewritten
 289 in such a way that powers n of the distance $R = |\vec{R}|$ are damped with a damping function
 290 $\lambda_n(\vec{u}(\vec{R}))$ [19].

291 There is a large number of fractional charge densities $\rho_f(\vec{u})$ that have been tested for the purpose
 292 of giving best results for the molecular polarizability as well as interaction energies. Note how a
 293 great advantage of the Thole model is the exceptional transferability of the atomic polarizabilities
 294 to compounds not used for the fitting procedure [17]. In fact, for most organic molecules, a fixed
 295 set of atomic polarizabilities ($\alpha_C = 1.334$, $\alpha_H = 0.496$, $\alpha_N = 1.073$, $\alpha_O = 0.873$, $\alpha_S = 2.926 \text{ \AA}^3$)
 296 based on atomic elements yields satisfactory results.

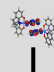
VOTCA implements the Thole model with an exponentially-decaying fractional charge density

$$\rho(u) = \frac{3a}{4\pi} \exp(-au^3), \quad (2.17)$$

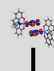
297 where $\vec{u}(\vec{R}, \alpha^a \alpha^b) = \vec{R}/(\alpha^a \alpha^b)^{1/6}$ and the smearing exponent $a = 0.39$ (which can however be
 298 changed from the program options), as used in the AMOEBA force field [19].

299 Even though the Thole model performs very well for many organic compounds with only the
 300 above small set of element-based polarizabilities, conjugated molecules may require a more in-
 301 tricate parametrization. The simplest approach is to resort to scaled polarizabilities to match

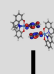
the effective molecular polarizable volume $V \sim \alpha_x \alpha_y \alpha_z$ as predicted by QM calculations (here $\alpha_x, \alpha_y, \alpha_z$ are the eigenvalues of the molecular polarizability tensor). The `molpol` tool assists with this task, it self-consistently calculates the Thole polarizability for an input `mps`-file and optimizes (if desired) the atomic polarizabilities in the above simple manner.

 **Generate Thole-type polarizabilities for a segment**
 | `xtp_tools -o options.xml -e molpol`

The electrostatic and induction contribution to the site energy is evaluated by the `emultipole` calculator. Atomistic partial charges for charged and neutral molecules are taken from `mps`-files (extended GDMA format) specified in `map.xml`. Note that, in order to speed up calculations for both methods, a cut-off radius (for the molecular centers of mass) can be given in `options.xml`. Threaded execution is advised.

 **Electrostatic and induction corrections**
 | `xtp_run -o options.xml -f state.sql -e emultipole`

Furthermore available are `zmultipole`, which extends `emultipole` to allow for an electrostatic buffer layer (loosely related to the `z`-buffer in OpenGL, hence the name) and anisotropic point polarizabilities. For the interaction energy of charged clusters of any user-defined composition (Frenkel states, CT states, ...), `xqmultipole` can be used.

 **Interaction energy of charged molecular clusters embedded in a molecular environment**
 | `xtp_parallel -o options.xml -f state.sql -e xqmultipole`

2.7 Transfer integrals

The electronic transfer integral element J_{ij} entering the Marcus rates in eq. (2.31) is defined as

$$J_{ij} = \langle \phi_i | \hat{H} | \phi_j \rangle, \quad (2.18) \quad \text{equ:TI}$$

where ϕ_i and ϕ_j are diabatic wavefunctions, localized on molecule i and j respectively, participating in the charge transfer, and \hat{H} is the Hamiltonian of the formed dimer. Within the frozen-core approximation, the usual choice for the diabatic wavefunctions ϕ_i is the highest occupied molecular orbital (HOMO) in case of hole transport, and the lowest unoccupied molecular orbital (LUMO) in the case of electron transfer, while \hat{H} is an effective single particle Hamiltonian, e.g. Fock or Kohn-Sham operator of the dimer. As such, J_{ij} is a measure of the strength of the electronic coupling of the frontier orbitals of monomers mediated by the dimer interactions.

Intrinsically, the transfer integral is very sensitive to the molecular arrangement, i.e. the distance and the mutual orientation of the molecules participating in charge transport. Since this arrangement can also be significantly influenced by static and/or dynamic disorder [20–24], it is essential to calculate J_{ij} explicitly for each hopping pair within a realistic morphology. Considering that the number of dimers for which eq. (2.18) has to be evaluated is proportional to the number of molecules times their coordination number, computationally efficient and at the same time quantitatively reliable schemes are required.

2.7.1 Projection of monomer orbitals on dimer orbitals (DIPRO)

An approach for the determination of the transfer integral that can be used for any single-particle electronic structure method (Hartree-Fock, DFT, or semiempirical methods) is based on the projection of monomer orbitals on a manifold of explicitly calculated dimer orbitals. This dimer projection (DIPRO) technique including an assessment of computational parameters such as the basis set, exchange-correlation functionals, and convergence criteria is presented in detail in ref. [25]. A brief summary of the concept is given below.

341 We start from an effective Hamiltonian ¹

$$\hat{H}^{\text{eff}} = \sum_i \epsilon_i \hat{a}_i^\dagger \hat{a}_i + \sum_{j \neq i} J_{ij} \hat{a}_i^\dagger \hat{a}_j + c.c. \quad (2.19) \quad \text{equ:dipro_eq1}$$

342 where \hat{a}_i^\dagger and \hat{a}_i are the creation and annihilation operators for a charge carrier located at the
 343 molecular site i . The electron site energy is given by ϵ_i , while J_{ij} is the transfer integral between
 344 two sites i and j . We label their frontier orbitals (HOMO for hole transfer, LUMO for electron
 345 transfer) ϕ_i and ϕ_j , respectively. Assuming that the frontier orbitals of a dimer (adiabatic energy
 346 surfaces) result exclusively from the interaction of the frontier orbitals of monomers, and conse-
 347 quently expand them in terms of ϕ_i and ϕ_j . The expansion coefficients, $\bar{\mathbf{C}}$, can be determined by
 348 solving the secular equation

$$(\mathbf{H} - E\mathbf{S})\bar{\mathbf{C}} = 0 \quad (2.20) \quad \text{equ:dipro_eq2}$$

349 where \mathbf{H} and \mathbf{S} are the Hamiltonian and overlap matrices of the system, respectively. These
 350 matrices can be written explicitly as

$$\mathbf{H} = \begin{pmatrix} e_i & H_{ij} \\ H_{ij}^* & e_j \end{pmatrix} \quad \mathbf{S} = \begin{pmatrix} 1 & S_{ij} \\ S_{ij}^* & 1 \end{pmatrix} \quad (2.21) \quad \text{equ:dipro_eq3}$$

351 with

$$\begin{aligned} e_i &= \langle \phi_i | \hat{H} | \phi_i \rangle & H_{ij} &= \langle \phi_i | \hat{H} | \phi_j \rangle \\ e_j &= \langle \phi_j | \hat{H} | \phi_j \rangle & S_{ij} &= \langle \phi_j | \phi_j \rangle \end{aligned} \quad (2.22) \quad \text{equ:dipro_eq4}$$

352 The matrix elements $e_{i(j)}$, H_{ij} , and S_{ij} entering eq. (2.21) can be calculated via projections on the
 353 dimer orbitals (eigenfunctions of \hat{H}) $\{|\phi_n^D\rangle\}$ by inserting $\hat{1} = \sum_n |\phi_n^D\rangle \langle \phi_n^D|$ twice. We exemplify
 354 this explicitly for H_{ij} in the following

$$H_{ij} = \sum_{nm} \langle \phi_i | \phi_n^D \rangle \langle \phi_n^D | \hat{H} | \phi_m^D \rangle \langle \phi_m^D | \phi_j \rangle. \quad (2.23) \quad \text{equ:dipro_eq16}$$

355 The Hamiltonian is diagonal in its eigenfunctions, $\langle \phi_n^D | \hat{H} | \phi_m^D \rangle = E_n \delta_{nm}$. Collecting the projec-
 356 tions of the frontier orbitals $|\phi_{i(j)}\rangle$ on the n -th dimer state $(\bar{\mathbf{V}}_{(i)})_n = \langle \phi_i | \phi_n^D \rangle$ and $(\bar{\mathbf{V}}_{(j)})_n =$
 357 $\langle \phi_j | \phi_n^D \rangle$ respectively, into vectors we obtain

$$H_{ij} = \bar{\mathbf{V}}_{(i)} \mathbf{E} \bar{\mathbf{V}}_{(j)}^\dagger. \quad (2.24) \quad \text{equ:dipro_eq17}$$

358 What is left to do is determine these projections $\bar{\mathbf{V}}_{(k)}$. In all practical calculations the molecular
 359 orbitals are expanded in basis sets of either plane waves or of localized atomic orbitals $|\varphi_\alpha\rangle$.
 360 We will first consider the case that the calculations for the monomers are performed using a
 361 counterpoise basis set that is commonly used to deal with the basis set superposition error (BSSE).
 362 The basis set of atom-centered orbitals of a monomer is extended to the one of the dimer by
 363 adding the respective atomic orbitals at virtual coordinates of the second monomer. We can then
 364 write the respective expansions as

$$|\phi_k\rangle = \sum_\alpha \lambda_\alpha^{(k)} |\varphi_\alpha\rangle \quad \text{and} \quad |\phi_n^D\rangle = \sum_\alpha D_\alpha^{(n)} |\varphi_\alpha\rangle \quad (2.25) \quad \text{equ:dipro_eq18}$$

365 where $k = i, j$. The projections can then be determined within this common basis set as

$$(\bar{\mathbf{V}}_k)_n = \langle \phi_k | \phi_n^D \rangle = \sum_\alpha \lambda_\alpha^{(k)} \langle \alpha | \sum_\beta D_\beta^{(n)} |\beta\rangle = \bar{\boldsymbol{\lambda}}_{(k)}^\dagger \mathbf{S} \bar{\mathbf{D}}_{(n)} \quad (2.26) \quad \text{equ:dipro_eq19}$$

¹we use following notations: a - number, $\bar{\mathbf{a}}$ - vector, \mathbf{A} - matrix, \hat{A} - operator

366 where \mathcal{S} is the overlap matrix of the atomic basis functions. This allows us to finally write the
 367 elements of the Hamiltonian and overlap matrices in eq. (2.21) as:

$$\begin{aligned} H_{ij} &= \bar{\lambda}_{(i)}^\dagger \mathcal{S} \mathbf{D} \mathbf{E} \mathcal{D}^\dagger \mathcal{S}^\dagger \bar{\lambda}_{(j)} \\ S_{ij} &= \bar{\lambda}_{(i)}^\dagger \mathcal{S} \mathbf{D} \mathbf{D}^\dagger \mathcal{S}^\dagger \bar{\lambda}_{(j)} \end{aligned} \quad (2.27) \quad \text{eq:dipro_eq20}$$

368 Since the two monomer frontier orbitals that form the basis of this expansion are not orthogonal
 369 in general ($\mathbf{S} \neq \mathbf{1}$), it is necessary to transform eq. (2.20) into a standard eigenvalue problem of
 370 the form

$$\mathbf{H}^{\text{eff}} \bar{\mathbf{C}}^{\text{eff}} = E \bar{\mathbf{C}}^{\text{eff}} \quad (2.28) \quad \text{eq:dipro_eq7}$$

371 to make it correspond to eq. (2.19). According to Löwdin such a transformation can be achieved
 372 by

$$\mathbf{H}^{\text{eff}} = \mathbf{S}^{-1/2} \mathbf{H} \mathbf{S}^{-1/2}. \quad (2.29) \quad \text{eq:dipro_eq9}$$

373 This then yields an effective Hamiltonian matrix in an orthogonal basis, and its entries can di-
 374 rectly be identified with the site energies ϵ_i and transfer integrals J_{ij} :

$$\mathbf{H}^{\text{eff}} = \begin{pmatrix} e_i^{\text{eff}} & H_{ij}^{\text{eff}} \\ H_{ij}^{*,\text{eff}} & e_j^{\text{eff}} \end{pmatrix} = \begin{pmatrix} \epsilon_i & J_{ij} \\ J_{ij}^* & \epsilon_j \end{pmatrix} \quad (2.30) \quad \text{eq:dipro_eq11}$$

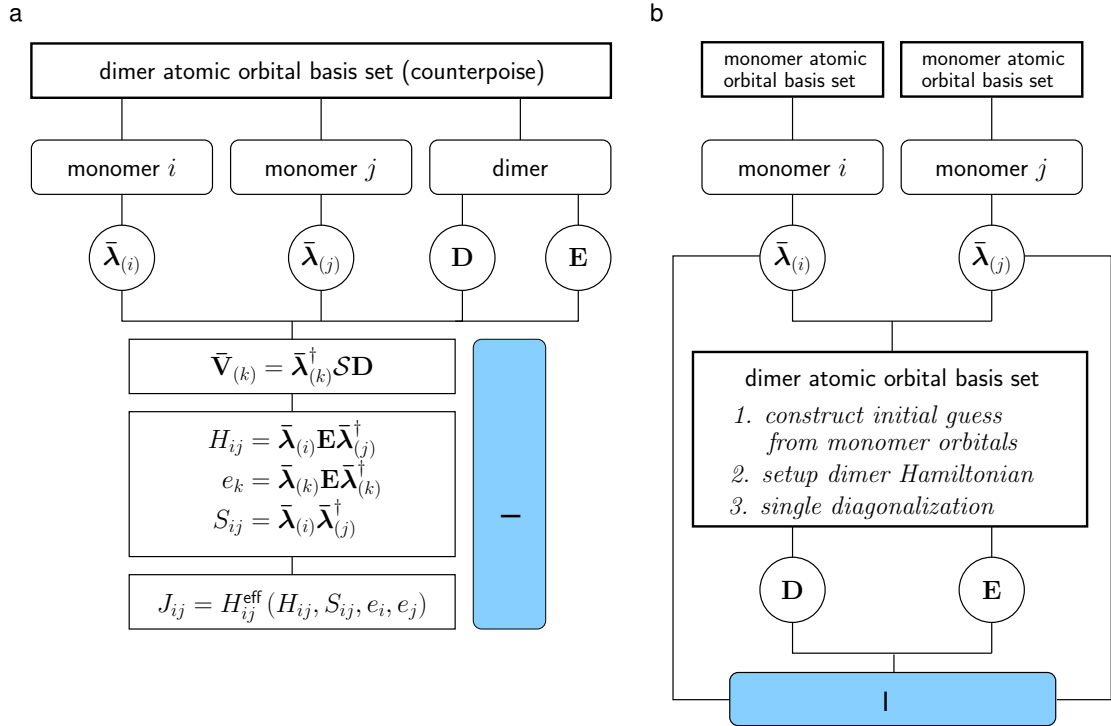


Figure 2.4: Schematics of the DIPRO method. (a) General workflow of the projection technique. (b) Strategy of the efficient noCP+noSCF implementation, in which the monomer calculations are performed independently from the dimer configurations (noCP), using the `edft calculator`. The dimer Hamiltonian is subsequently constructed based on an initial guess formed from monomer orbitals and only diagonalized once (noSCF) before the transfer integral is calculated by projection. This second step is performed by the `idft calculator`.

2.7.2 DFT-based transfer integrals using DIPRO

The calculation of one electronic coupling element based on DFT using the DIPRO method requires the overlap matrix of atomic orbitals \mathcal{S} , the expansion coefficients for monomer $\bar{\lambda}^{(k)} = \{\lambda_{\alpha}^{(k)}\}$ and dimer orbitals $\bar{D}^{(n)} = \{D_{\alpha}^{(n)}\}$, as well as the orbital energies E_n of the dimer are required as input. In practical situations, performing self-consistent quantum-chemical calculations for each individual monomer and one for the dimer to obtain this input data is extremely demanding. Several simplifications can be made to reduce the computational effort, such as using non-Counterpoise basis sets for the monomers (thereby decoupling the monomer calculations from the dimer run) and performing only a single SCF step in a dimer calculation starting from an initial guess formed from a superposition of monomer orbitals. This "noCP+noSCF" variant of DIPRO is shown in figure 2.4(a) and recommended for production runs. A detailed comparative study of the different variants can be found in [25].

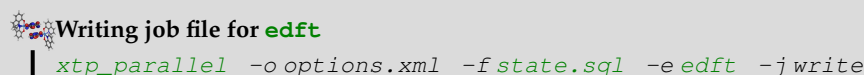
The code currently contains supports evaluation of transfer integrals from quantum-chemical calculations performed with the Gaussian, Turbomole, and NWChem packages. The interfacing procedure consists of three main steps: generation of input files for monomers and dimers, performing the actual quantum-chemical calculations, and calculating the transfer integrals.

Monomer calculations

First, **hopping sites** and a **neighbor list** need to be generated from the atomistic topology and trajectory and written to the `state.sql` file. Then the parallel **edft calculator** manages the calculation of the monomer properties required for the determination of electronic coupling elements. Specifically, the individual steps it performs are:

1. Creation of a job file containing the list of molecules to be calculated with DFT

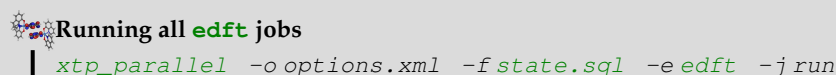
```


Writing job file for edft
| xtp_parallel -o options.xml -f state.sql -e edft -j write

```

2. Running of all jobs in job file

```


Running all edft jobs
| xtp_parallel -o options.xml -f state.sql -e edft -j run

```

which includes

- creating the input files for the DFT calculation (using the package specified in `options.xml`) in the directory

```
OR_FILES/package/frame_F/mol_M
```

where F is the index of the frame in the trajectory, M is the index of a molecule in this frame,

- executing the DFT run, and
- after completion of this run, parsing the output (number of electrons, basis set, molecular orbital expansion coefficients), and saving it in compressed form to

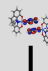
```
OR_FILES/molecules/frame_F/molecule_M.orb
```

Calculating the transfer integrals

After the monomer calculations have been completed successfully, the respective runs for dimers from the neighborlist can be performed using the parallel **idft calculator**, which manages the DFT runs for the hopping pairs and determines the coupling element using DIPRO. Again, several steps are required:

- 415 1. Creation of a job file containing the list of pairs to be calculated with DFT

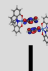
```

 Writing job file for idft
| xtp_parallel -o options.xml -f state.sql -e idft -j write

```

- 417 2. Running of all jobs in job file

```

 Running all idft jobs
| xtp_parallel -o options.xml -f state.sql -e idft -j run

```

418 which includes

- 420 • creating the input files (including the merged guess for a noSCF calculation, if re-
- 421 requested) for the DFT calculation (using the package specified in `options.xml`) in the
- 422 directory

423 `OR_FILES/package/frame_F/pair_M_N`

424 where M and N are the indices of the molecules in this pair,

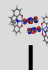
- 425 • executing the DFT run, and
- 426 • after completion of this run, parsing the output (number of electrons, basis set, molec-
- 427 ular orbital expansion coefficients and energies, atomic orbital overlap matrix), and
- 428 saving the pair information in compressed form to

429 `OR_FILES/pairs/frame_F/pair_M_N.orb`

- 430 • loading the monomer orbitals from the previously saved `*.orb` files.
- 431 • calculating the coupling elements and write them to the job file

- 432 3. Reading the coupling elements from the job file and saving them to the `state.sql` file

```

 Saving idft results from job file to state.sql
| xtp_parallel -o options.xml -f state.sql -e idft -j read

```

434 2.7.3 ZINDO-based transfer integrals using MOO

sec:zindo

435 An approximate method based on Zerner's Intermediate Neglect of Differential Overlap (ZINDO)
 436 has been described in Ref. [26]. This semiempirical method is substantially faster than first-
 437 principles approaches, since it avoids the self-consistent calculations on each individual monomer
 438 and dimer. This allows to construct the matrix elements of the ZINDO Hamiltonian of the dimer
 439 from the weighted overlap of molecular orbitals of the two monomers. Together with the in-
 440 troduction of rigid segments, only a single self-consistent calculation on one isolated conjugated
 441 segment is required. All relevant molecular overlaps can then be constructed from the obtained
 442 molecular orbitals.

443 The main advantage of the molecular orbital overlap (MOO) library is *fast* evaluation of electronic
 444 coupling elements. Note that MOO is based on the ZINDO Hamiltonian which has limited appli-
 445 cability. The general advice is to first compare the accuracy of the MOO method to the DFT-based
 446 calculations.

447 MOO can be used both in a **standalone mode** and as an **izindo calculator** of VOTCA-XTP.

448 Since MOO constructs the Fock operator of a dimer from the molecular orbitals of monomers by
 449 translating and rotating the orbitals of **rigid fragments**, the optimized geometry of all **conjugated**
 450 **segments** and the coefficients of the molecular orbitals are required as its input in addition to
 451 the state file (`state.sql`) with the **neighbor list**. Coordinates are stored in `geometry.xyz`
 452 files with four columns, first being the atom type and the next three atom coordinates. This is a
 453 standard `xyz` format without a header. Note that the atom order in the `geometry.xyz` files can

454 be different from that of the mapping files. The correspondence between the two is established
455 in the `map.xml` file.



Be careful!

Izindo requires the specification of orbitals for hole and electron transport in `map.xml`. They are the HOMO and LUMO respectively and can be retrieved from the `log` file from which the `zindo.orb` file is generated. The number of alpha electrons is the HOMO, the LUMO is HOMO+1

456

457

The calculated transfer integrals are immediately saved to the `state.sql` file.



Transfer integrals from izindo

```
xtp_run -o options.xml -f state.sql -e izindo
```

458

2.8 Charge transfer rate

sec:rates

460

461

462

463

464

Charge transfer rates can be postulated based on intuitive physical considerations, as it is done in the Gaussian disorder models [20, 27–29]. Alternatively, charge transfer theories can be used to evaluate rates from quantum chemical calculations [1, 8, 25, 30–32]. In spite of being significantly more computationally demanding, the latter approach allows to link the chemical and electronic structure, as well as the morphology, to charge dynamics.

2.8.1 Classical charge transfer rate

sec:rate_classical

466

467

468

469

The high temperature limit of classical charge transfer theory [33, 34] is often used as a trade-off between theoretical rigor and computational complexity. It captures key parameters which influence charge transport while at the same time providing an analytical expression for the rate. Within this limit, the transfer rate for a charge to hop from a site i to a site j reads

$$\omega_{ij} = \frac{2\pi}{\hbar} \frac{J_{ij}^2}{\sqrt{4\pi\lambda_{ij}k_{\text{B}}T}} \exp\left[-\frac{(\Delta E_{ij} - \lambda_{ij})^2}{4\lambda_{ij}k_{\text{B}}T}\right], \quad (2.31) \quad \text{equ:marcus}$$

470

471

472

where T is the temperature, $\lambda_{ij} = \lambda_{ij}^{\text{int}} + \lambda_{ij}^{\text{out}}$ is the **reorganization energy**, which is a sum of intra- and inter-molecular (outersphere) contributions, ΔE_{ij} is the **site-energy difference**, or driving force, and J_{ij} is the **electronic coupling element**, or transfer integral.

2.8.2 Semi-classical bimolecular rate

sec:rate_bimolecular

474

475

476

477

478

479

480

481

482

483

The main assumptions in eq. (2.31) are non-adiabaticity (small electronic coupling and charge transfer between two diabatic, non-interacting states), and harmonic promoting modes, which are treated classically. At ambient conditions, however, the intramolecular promoting mode, which roughly corresponds to C-C bond stretching, has a vibrational energy of $\hbar\omega \approx 0.2 \text{ eV} \gg k_{\text{B}}T$ and should be treated quantum-mechanically. The outer-sphere (slow) mode has much lower vibrational energy than the intramolecular promoting mode, and therefore can be treated classically. The weak interaction between molecules also implies that each molecule has its own, practically independent, set of quantum mechanical degrees of freedom.

A more general, quantum-classical expression for a bimolecular multi-channel rate is derived in the Supporting Information of ref. [1] and has the following form

$$\omega_{ij} = \frac{2\pi}{\hbar} \frac{|J_{ij}|^2}{\sqrt{4\pi\lambda_{ij}^{\text{out}}k_{\text{B}}T}} \sum_{l', m'=0}^{\infty} |\langle \chi_{i0}^c | \chi_{il'}^n \rangle|^2 |\langle \chi_{j0}^n | \chi_{jm'}^c \rangle|^2 \exp\left\{-\frac{[\Delta E_{ij} - \hbar(l'\omega_i^n + m'\omega_j^c) - \lambda_{ij}^{\text{out}}]^2}{4\lambda_{ij}^{\text{out}}k_{\text{B}}T}\right\}. \quad (2.32) \quad \text{equ:jjortner}$$

If the curvatures of intramolecular PES of charged and neutral states of a molecule are different, that is $\omega_i^c \neq \omega_i^n$, the corresponding reorganization energies, $\lambda_i^{cn} = \frac{1}{2}[\omega_i^n(q_i^n - q_i^c)]^2$ and $\lambda_i^{nc} = \frac{1}{2}[\omega_i^c(q_i^n - q_i^c)]^2$, will also differ. In this case the Franck-Condon (FC) factors for discharging of molecule i read [35]

$$|\langle \chi_{i0}^c | \chi_{il'}^n \rangle|^2 = \frac{2}{2^{l'} l'! (\omega_i^c + \omega_i^n)} \exp(-|s_i|) \left[\sum_{\substack{l'=0 \\ k \text{ even}}}^{l'} \binom{l'}{k} \left(\frac{2\omega_i^c}{\omega_i^c + \omega_i^n} \right)^{k/2} \frac{k!}{(k/2)!} H_{l'-k} \left(\frac{s_i}{\sqrt{2S_i^{cn}}} \right) \right]^2, \quad (2.33)$$

484 where $H_n(x)$ is a Hermite polynomial, $s_i = 2\sqrt{\lambda_i^{nc}\lambda_i^{cn}}/\hbar(\omega_i^c + \omega_i^n)$, and $S_i^{cn} = \lambda_i^{cn}/\hbar\omega_i^c$. The FC
485 factors for charging of molecule j can be obtained by substituting $(s_i, S_i^{cn}, \omega_i^c)$ with $(-s_j, S_j^{nc}, \omega_j^n)$.
486 In order to evaluate the FC factors, the **internal reorganization energy** λ_i^{cn} can be computed from
487 the intramolecular PES.

488 2.8.3 Semi-classical rate

sec:rate_semiclassical

One can also use the quantum-classical rate with a common set of vibrational coordinates [9]

$$\omega_{ij} = \frac{2\pi}{\hbar} \frac{|J_{ij}|^2}{\sqrt{4\pi\lambda_{ij}^{\text{out}}k_B T}} \sum_{N=0}^{\infty} \frac{1}{N!} \left(\frac{\lambda_{ij}^{\text{int}}}{\hbar\omega^{\text{int}}} \right)^N \exp\left(-\frac{\lambda_{ij}^{\text{int}}}{\hbar\omega^{\text{int}}}\right) \exp\left\{-\frac{[\Delta E_{ij} - \hbar N\omega^{\text{int}} - \lambda_{ij}^{\text{out}}]^2}{4\lambda_{ij}^{\text{out}}k_B T}\right\}. \quad (2.34)$$

equ:ortner

489 Numerical estimates show that if $\lambda_{ij}^{\text{int}} \approx \lambda_{ij}^{\text{out}}$ and $|\Delta E_{ij}| \ll \lambda_{ij}^{\text{out}}$ the rates are similar to those of
490 eq. (2.31). In general, there is no robust method to compute $\lambda_{ij}^{\text{out}}$ [36] and both reorganization
491 energies are often assumed to be of the same order of magnitude. In this case the second condi-
492 tion also holds, unless there are large differences in electron affinities or ionization potentials of
493 neighboring molecules, e.g. in donor-acceptor blends.

494 To calculate rates of the type specified in `options.xml` for all pairs in the **neighbor list** and to
495 save them into the `state.sql` file, run the **rates calculator**. Note that all required ingredients
496 (**reorganization energies**, **transfer integrals**, and **site energies** have to be calculated before).



Calculation of transfer rates

```
| xtp_run -o options.xml -f state.sql -e rates
```

497

498 2.9 Master equation

sec:kmc

499 Having determined the list of conjugated segments (hopping sites) and charge transfer rates be-
500 tween them, the next task is to solve the master equation which describes the time evolution of
501 the system

$$\frac{\partial P_\alpha}{\partial t} = \sum_{\beta} P_\beta \Omega_{\beta\alpha} - \sum_{\beta} P_\alpha \Omega_{\alpha\beta}, \quad (2.35)$$

equ:master

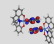
502 where P_α is the probability of the system to be in a state α at time t and $\Omega_{\alpha\beta}$ is the transition rate
503 from state α to state β . A state α is specified by a set of site occupations, $\{\alpha_i\}$, where $\alpha_i = 1(0)$
504 for an occupied (unoccupied) site i , and the matrix $\hat{\Omega}$ can be constructed from rates ω_{ij} .

505 The solution of eq. (2.35) is obtained by using kinetic Monte Carlo (KMC) methods. KMC
506 explicitly simulates the dynamics of charge carriers by constructing a Markov chain in state space
507 and can find both stationary and transient solutions of the master equation. The main advantage
508 of KMC is that only states with a direct link to the current state need to be considered at each step.
509 Since these can be constructed solely from current site occupations, extensions to multiple charge

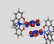
510 carriers (without the mean-field approximation), site-occupation dependent rates (needed for
 511 the explicit treatment of Coulomb interactions), and different types of interacting particles and
 512 processes, are straightforward. To optimize memory usage and efficiency, a combination of the
 513 variable step size method [37] and the first reaction method is implemented.

514 To obtain the dynamics of charges using KMC, the program `xtp_kmc_run` executes a specific
 515 `calculator` after reading its options (charge carrier type, runtime, numer of carriers etc.) from
 516 `options.xml`.

```

517  KMC for a single carrier in periodic boundary conditions
    | xtp_kmc_run -o options.xml -f state.sql -e kmcsingle
  
```

```

518  KMC for multiple carriers of the same type in periodic boundary conditions
    | xtp_kmc_run -o options.xml -f state.sql -e kmcmultiple
  
```

519 2.9.1 Extrapolation to nondispersive mobilities

sec:nondispersive

520 Predictions of charge-carrier mobilities in partially disordered semiconductors rely on charge
 521 transport simulations in systems which are only several nanometers thick. As a result, simu-
 522 lated charge transport might be dispersive for materials with large energetic disorder [38, 39]
 523 and simulated mobilities are system-size dependent. In time-of-flight (TOF) experiments, how-
 524 ever, a typical sample thickness is in the micrometer range and transport is often nondispersive.
 525 In order to link simulation and experiment, one needs to extract the nondispersive mobility from
 526 simulations of small systems, where charge transport is dispersive at room temperature.

527 Such extrapolation is possible if the temperature dependence of the nondispersive mobility is
 528 known in a wide temperature range. For example, one can use analytical results derived for one-
 529 dimensional models [40–42]. The mobility-temperature dependence can then be parametrized by
 530 simulating charge transport at elevated temperatures, for which transport is nondispersive even
 531 for small system sizes. This dependence can then be used to extrapolate to the nondispersive
 532 mobility at room temperature [43].

533 For Alq₃, the charge carrier mobility of a periodic system of 512 molecules was shown to be
 534 more than three orders of magnitude higher than the nondispersive mobility of an infinitely
 535 large system [43]. Furthermore, it was shown that the transition between the dispersive and
 536 nondispersive transport has a logarithmic dependence on the number of hopping sites N . Hence,
 537 a brute-force increase of the system size cannot resolve the problem for compounds with large
 538 energetic disorder σ , since N increases exponentially with σ^2 .

539 2.10 Stochastic Networks

sec:stochastic

540 The VOTCA package contains the functionality of generating large, amorphous charge transport
 541 networks ($\sim 10^6$ molecules). This is done with a combined coarse-grained and stochastic ap-
 542 proach. VOTCA::CSG is used to generate a coarse-grained morphology. The stochastic modeling
 543 of VOTCA::CTP allows to make a charge transfer network out of this morphology by reproduc-
 544 ing the neighbor list (connectivity), transfer integrals, correlated site energies. An overview is
 545 given in Figure 2.5.

546 Throughout this section we will use two state files. One is the state file `state_ref.sql` of the
 547 smaller reference system that can be generated as explained in the previous sections. The second
 548 one is the state file `state_cg.sql` of the coarse-grained system, or the stochastic network, that
 549 can be parametrized as explained in this section.

550 When using the stochastic functionalities, please cite the corresponding work:

- 551 1. B. Baumeier, O. Stenzel, C. Poelking, D. Andrienko, and V. Schmidt: Stochastic modeling of
 552 molecular charge transport networks. Phys. Rev. B 86, 184202 (2012)

- 553 2. P. Kordt and D. Andrienko: Modeling of Spatially Correlated Energetic Disorder in Organic
554 Semiconductors. *Journal of Chemical Theory and Computation* 12, 36–40 (2016)
- 555 3. P. Kordt, J. J. M. van der Holst, M. Al Helwi, W. Kowalsky, F. May, A. Badinski, C. Lennartz,
556 and D. Andrienko: Modeling of Organic Light Emitting Diodes: From Molecular to Device
557 Properties. *Advanced Functional Materials* 25, 1955–1971 (2015)

MORPHOLOGY		
	EXTRACT	REPRODUCE
RDF and coarse grained potential	GROMACS g_rdf -f traj.xtc -s topol.tpr	VOTCA::CSG csg_inverse -options settings.xml
morphology		GROMACS mdrun

RATES		
	EXTRACT	REPRODUCE
neighbor list (pairs)	xtp_run -e panalyze -o options.xml -f state_reference.sql	xtp_run -e neighborlist -o options.xml -f state_cg.sql
site energies	xtp_run -e eanalyze -o options.xml -f state_reference.sql	xtp_run -e eimport -o options.xml -f state_cg.sql
transfer integrals	xtp_run -e ianalyze -o options.xml -f state_reference.sql	xtp_run -e iimport -o options.xml -f state_cg.sql
rates	not used directly	xtp_run -e rates -o options.xml -f state_cg.sql

Figure 2.5: Stochastic Model in VOTCA. Overview of the different steps for generating stochastic charge transport networks in VOTCA. The Molecular Dynamics software GROMACS allows to analyze the radial distribution function of a morphology, which is then used by VOTCA::CSG to generate a coarse-grained potential that reproduces this distribution function. This potential can then be used for coarse-grained simulations in GROMCAS. For calculating rates in the coarse-grained morphology, first the relevant parameters are extracted (panalyze, eanalyze, ianalyze) from the reference morphology and then reproduced in the coarse-grained morphology (neighborlist, eimport, iimport). With all these at hand, the rates calculator can be used in the coarse-grained morphology.

fig:overview_stochastic

558 2.10.1 Coarse-grained morphology

559 The first step is to generate a coarse-grained morphology. In this example, it is done by mapping
560 a DPBIC molecule (which consists of 103 atoms) to a single point, its center of mass and by using

561 the iterative Boltzmann inversion (IBI) method. Starting point is a smaller reference morphology,
562 generated with GROMACS. Using the command

```
563 g_rdf -f traj.xtc -s topol.tpr
```

564 you can extract the radial distribution function $g(r)$ of your reference topology, outputted into the
565 file `rdf.xvg`. This file, together with `table.xvg`, `grompp.mdp`, `topol.top`, `index.ndx` and `confout.gro`
566 form your reference data.

567 For VOTCA::CSG you need a **setting.xml** file:

```
568 <cg>
569 <!-- example for a non-bonded interaction entry -->
570 <non-bonded>
571 <!-- name of the interaction -->
572 <name>IR-IR</name>
573 <!-- types involved in this interaction -->
574 <type1>IR</type1>
575 <type2>IR</type2>
576 <!-- dimension + grid spacing of tables for calculations -->
577 <min>0.5</min>
578 <max>5.0</max>
579 <step>0.01</step>
580 <inverse>
581 <!-- target distribution (rdf), just give gromacs rdf.xvg -->
582 <target>rdf.xvg</target>
583 <!-- update cycles -->
584 <do_potential>1</do_potential>
585 <!-- additional post processing of dU before added to potential -->
586 <post_update>scale smooth</post_update>
587 <post_update_options>
588 <scale>0.5</scale> <!--Scale the potential before updating it -->
589 <smooth>
590 <iterations>2</iterations>
591 </smooth>
592 </post_update_options>
593 <!-- additional post processing of U after dU added to potential -->
594 <post_add></post_add>
595 <!-- name of the table for gromacs run -->
596 <gromacs>
597 <table>table_IR_IR.xvg</table>
598 </gromacs>
599 </inverse>
600 </non-bonded>
601
602 <!-- general options for inverse script -->
603 <inverse>
604 <!-- 300*0.00831451 gromacs units -->
605 <kBT>2.49435300</kBT>
606 <initial_configuration>maindir</initial_configuration>
607 <!-- use gromacs as simulation program -->
608 <program>gromacs</program>
609 <!-- gromacs specific options -->
610 <gromacs>
611 <!-- trash so many frames at the beginning -->
612 <equi_time>500</equi_time>
613 <!-- grid for table*.xvg !-->
614 <table_bins>0.001</table_bins>
615 <!-- cut the potential at this value (gromacs bug) -->
616 <pot_max>1000000</pot_max>
617 <!-- extend the tables to this value -->
618
```

```

619     <table_end>6.0</table_end>
620 </gromacs>
621 <!-- these files are copied for each new run -->
622 <filelist>grompp.mdp topol.top index.ndx table.xvg</filelist>
623 <!-- do so many iterations -->
624 <iterations_max>500</iterations_max>
625 <!-- Try to clean a bit -->
626 <cleanlist>traj.xtc</cleanlist>
627 <!-- ibm: inverse boltzmann imc: inverse monte carlo -->
628 <method>ibi</method>
629 <!-- write log to this file -->
630 <log_file>inverse.log</log_file>
631 <!-- write restart step to this file -->
632 <restart_file>restart_points.log</restart_file>
633 <!-- imc specific stuff -->
634 </inverse>
635 </cg>
636

```

637 You run IBI using the command

```
638 csg_inverse -options settings.xml
```

639 IBI intends to find a potential $U(r)$ that reproduces your radial distribution function. It is stored
640 in the file **table_IR_IR.xvg** in our example.

641 With the interaction potential at hand, a large topology can be generated using molecular dy-
642 namics simulations for the coarse grained model. Starting point is a box with equally distributed
643 points, with each point representing one molecule and with the number of points chosen such
644 that the density of the reference system is reproduced. A small python script can generate the
645 conf.gro to start from, here shown to obtain a $50 \times 50 \times 120 \text{ nm}^3$ starting morphology.

```

646
647
648 from pylab import *
649 import numpy as np
650
651 lenX      = 50
652 lenY      = 50
653 lenZ      = 120
654 originalV = 4704.339
655 originalN = 4000
656 spacing   = (originalV/originalN)**(1./3.)
657
658 molecule  = "DPBIC"
659 resname   = "IRI"
660 atomname  = "IR"
661
662 newV = lenX*lenY*lenZ
663 newN = int(newV/originalV*originalN)
664
665 nX = int(lenX/spacing)+1
666 nY = int(lenY/spacing)+1
667 nZ = int(lenZ/spacing)+1
668
669 print "max. molecules in X direction: "+str(nX)
670 print "max. molecules in Y direction: "+str(nY)
671 print "max. molecules in Z direction: "+str(nZ)
672 print "total number of molecules: "+str(newN)
673
674 file = open("box.gro", "w")
675 file.write(molecule+"\n")
676 file.write(str(newN)+"\n")

```

```

677 atomnumber = 1
678 for iX in range(nX):
679     for iY in range(nY):
680         for iZ in range(nZ):
681             if(atomnumber > newN):
682                 break
683             posX = spacing*iX
684             posY = spacing*iY
685             posZ = spacing*iZ
686             print >> file, "%5d%-5s%5s%5d%8.3f%8.3f%8.3f%8.4f%8.4f%8.4f" % \
687                 (1, rename, atomname, 1, posX, posY, posZ, 0, 0, 0)
688             atomnumber += 1
689
690
691
692 file.write(" "+str(lenX)+" "+str(lenY)+" "+str(lenZ))
693 file.close()
694
695 print "Note: for some obscure reason VMD will not be able to read this file\
696 properly unless you open it once in vi and save it."
697

```

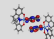
698 Open the box.gro in vi and save it (:wq), afterwards you can have a look at it in VDM. Run your
699 MD simulations using the mdrun command. In the end you can compare the radial distribution
700 functions of your reference and coarse-grained system, as shown in figure 2.6(a) as an example.

701 2.10.2 Charge transport network

702 To generate a charge transport network you first need a reference system with neighbor list, site
703 energies and transfer integrals calculated and stored in a **state.sql** state file. The procedure for all
704 these three properties is always the same: first analyze the reference data, and second import the
705 analyzation files and reproduce the properties.

706 Neighbor list

707 In the atomistic reference system molecules are connected if their two closest segments are below
708 a certain cut-off radius. This finer picture of segments does not exist in the coarse-grained system,
709 where each molecule is represented by a point. To mimick the neighbor list, the probability of
710 two molecules to be connected is analyzed as a function of their center-of-mass distance. This
711 can be done by using the *panalyze* calculator

 **Analyze the pair connectivity (neighborlist) in the reference system**

```
| xtp_run -o options.xml -f state_ref.sql -e panalyze
```

712 with the options defined as follows:

715 options_analyze.xml

```

716 <options>
717     <panalyze>
718         <resolution_space>0.05</resolution_space>
719     </panalyze>
720 </options>
721
722

```

723 The only parameter needed is the spacial resolution, i.e., the bin size for calculating the probabil-
724 ities. The *panalyze* calculator outputs a file **panalyze.distanceprobability.out** with the respective
725 probabilities. Now this file has to be imported into the coarse-grained state file

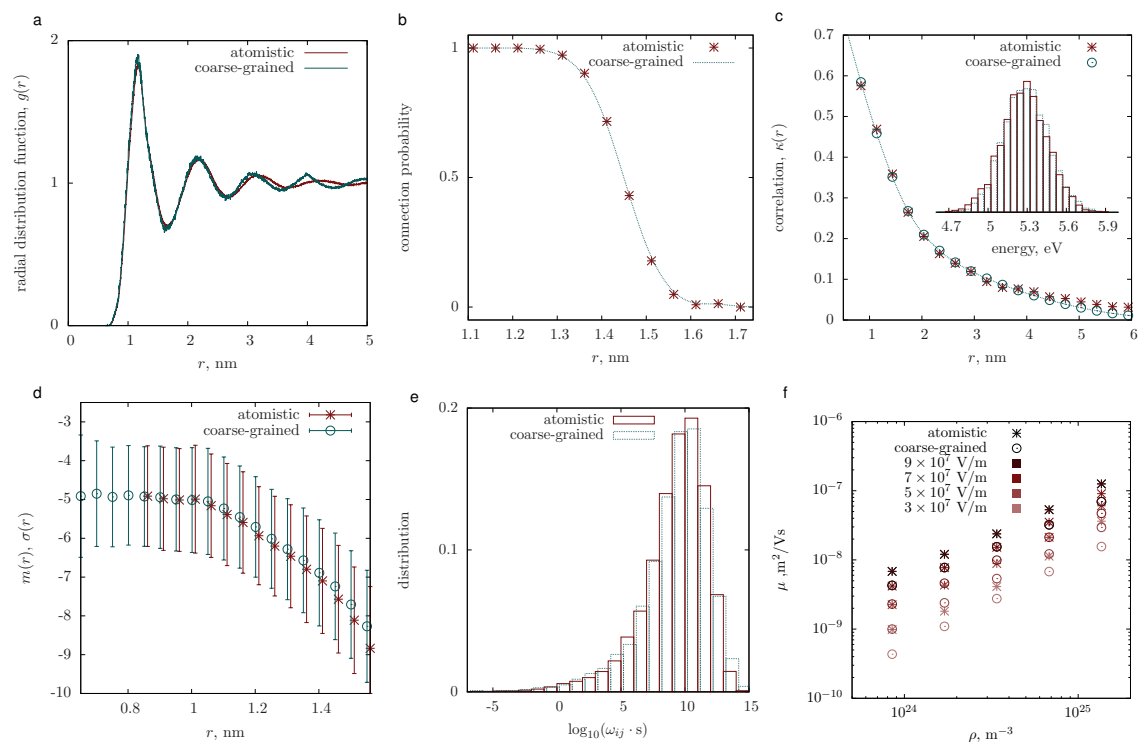
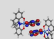


Figure 2.6: Comparison of the atomistic ($17 \times 17 \times 17 \text{ nm}^3$) and coarse-grained ($50 \times 50 \times 120 \text{ nm}^3$) models. (a) Radial distribution function, $g(r)$. (b) Probability of two sites to be connected (added to the neighbor list) as a function of their separation. (c) Spatial site energy autocorrelation function, $\kappa(r)$; Inset: Site energy distribution. (d) Mean m and width σ of a distribution of the logarithm of electronic couplings, $\log_{10}(J^2/\text{eV}^2)$, for molecules at a fixed separation r . (e) Rate distributions. (f) Mobility as a function of hole density, plotted for four different electric fields.

fig:stochastic

 Import the reference pair connectivity (neighborlist) and reproduce it in stochastic network

```
| xtp_run -o options.xml -f state_cg.sql -e neighborlist
```

726

using the following options:

727

728

options_import.xml

729

730

731

732

733

734

735

736

```
<options>
  <neighborlist>
    <probabilityfile>panalyze.distanceprobability.out</probabilityfile>
  </neighborlist>
</options>
```

737

738

739

740

For testing purposes, you can run the *panalyze* calculator on your coarse-grained state file and compare the probability function to the reference. An example is shown in figure 2.6(b). You can also look at the file **panalyze.distanceprobability.out** for both state files, which has the distribution of coordination numbers (number of neighbors) and its average in.

741

Site energies

742

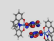
743

744

Site energies in amorphous organic semiconductors are roughly Gaussian distributed, with the width of the Gaussian, σ , called the energetic disorder. However, there are correlations between sites if they are close enough to each other. The aim in this section is therefore to reproduce the

745 correlated energetic landscape. The first step is to get a spatial correlation function as well as the
 746 mean energy and the energetic disorder from your reference state file:

747


Analyze the energy distribution and correlation in the reference system

```
| xtp_run -o options.xml -f state_ref.sql -e eanalyze
```

748

749 with the following options:

750

751 **options_analyze.xml**

752

```
753 <options>
754   <eanalyze>
755     <resolution_sites>0.05</resolution_sites>
756     <resolution_pairs>0.05</resolution_pairs>
757     <resolution_space>0.3</resolution_space>
758     <states>1,-1</states> <!-- +1 for hole transport, -1 for electron transport -->
759     <distancemode>centreofmass</distancemode>
760   </eanalyze>
761 </options>
```

763 The first three parameters determine bin sizes, then you can choose to look at hole and/or elec-
 764 tron energy. The keyword *centreofmass* means, that the correlation function is calculated as a
 765 function of the centre-of-mass distance of molecules and not as a function of their nearest seg-
 766 ments. For the stochastic simulations you always have to use the *centreofmass* mode!

767 The output files of this calculator that we need are **eanalyze.sitecorr_e.out** (for electrons) and
 768 **eanalyze.sitecorr_h.out** (for holes). In the second line of this file, you find mean and sigma of the
 769 energy distribution, as well as the mean of the static energies (without induction):

770

```
771 # EANALYZE: SPATIAL SITE-ENERGY CORRELATION
772 # AVG -0.4412655 STD 0.1739638 MIN_R 0.8365040 MAX_R 14.4771496 AVGESTATIC
773 -0.4730655
774 ...
```

775 These values have to be inserted manually into the options file for importing to the coarse-
 776 grained system (see below). Apart from that, the file contains the spatial correlation function.

777

778 You generate energies following this distribution and correlation by using the *eimport* calculator

Import the energy distribution and correlation and reproduce it in stochastic network

```
| xtp_run -o options.xml -f state_ref.sql -e eimport
```

779

780 with the options:

781

782 **options_import.xml**

783

```
784 <options>
785   <eimport>
786     <probabilityfile_h>reference/eanalyze.sitecorr_h.out</probabilityfile_h>
787     <sigma_h>0.1763163</sigma_h>
788     <avgestatic_h>-0.5913265</avgestatic_h>
789     <probabilityfile_e>reference/eanalyze.sitecorr_e.out</probabilityfile_e>
790     <sigma_e>0.1739638</sigma_e>
791     <avgestatic_e>-0.4730655</avgestatic_e>
792     <cutoff>8.5</cutoff>
793     <seed>1</seed>
794   </eimport>
795 </options>
```

796

797 The *cutoff* keyword can be used to read in the correlation function only up to a certain distance,
798 which can be useful if larger distances yield unphysical results.

799 Transfer Integrals

800 The last ingredient reproduced by the stochastic approach are transfer integrals J . The idea is that
801 $\log_{10}(J^2/\text{eV}^2)$ is roughly Gaussian distributed, with mean and error of the distribution varying
802 with distance (see figure 2.6 (d)). Use the calculator

 **Analyze the distance-dependent distribution of transfer integrals in the reference system**

```
| xtp_run -o options.xml -f state_ref.sql -e ianalyze
```

804 with options

805 options_analyze.xml

```
806
807 <options>
808   <ianalyze>
809     <resolution_logJ2>0.05</resolution_logJ2>
810     <resolution_space>0.05</resolution_space>
811     <states>1,-1</states> <!-- +1 for hole transport, -1 for electron transport -->
812   </ianalyze>
813 </options>
```

817 That will generate the files **ianalyze.ispatial_e.out** and **ianalyze.ispatial_h.out**, which contain
818 means and errors as a function of centre-of-mass distance.

819 Now use the *iimport* calculator to generate transfer integrals in the coarse grained state file, fol-
820 lowing the same statistics.

 **Import distance dependent distribution of transfer integrals and reproduce in stochastic network**

```
| xtp_run -o options.xml -f state_cg.sql -e iimport
```

822 options_import.xml

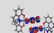
```
823
824 <options>
825   <iimport>
826     <TI_tag></TI_tag>
827     <TI_file></TI_file>
828     <idft_jobs_file></idft_jobs_file>
829     <probabilityfile_h>reference/ianalyze.ispatial_h.out</probabilityfile_h>
830     <probabilityfile_e>reference/ianalyze.ispatial_e.out</probabilityfile_e>
831   </iimport>
832 </options>
```

835 einternal

836 Run the *einternal* calculator, just as you do it for the reference system.

837 Rates

838 If you followed the steps in this section, you have everything at hand to calculate charge transfer
839 rates for the coarse grained system from the stochastic ingredients:

 **Calculate rates in the stochastic network**

```
| xtp_run -o options.xml -f state_cg.sql -e rates
```

840

Options are the same as for the reference file. You can check the result by comparing rates from your reference to the coarse-grained system, see figure 2.6(e) for an example. The resulting charge transport network can be used for kinetic Monte Carlo simulations with VOTCA. If everything goes well, mobilities for both systems should agree, as shown in figure 2.6(f).

2.11 Macroscopic observables

sec:analysis

Spatial distributions of charge and current densities can provide a better insight in the microscopic mechanisms of charge transport. If O is an observable which has a value O_α in a state α , its ensemble average at time t is a sum over all states weighted by the probability P_α to be in a state α at time t

$$\langle O \rangle = \sum_{\alpha} O_{\alpha} P_{\alpha}. \quad (2.36) \quad \text{equ:ensemble}$$

If O does not explicitly depend on time, the time evolution of $\langle O \rangle$ can be calculated as

$$\frac{d\langle O \rangle}{dt} = \sum_{\alpha, \beta} [P_{\beta} \Omega_{\beta\alpha} - P_{\alpha} \Omega_{\alpha\beta}] O_{\alpha} = \sum_{\alpha, \beta} P_{\beta} \Omega_{\beta\alpha} [O_{\alpha} - O_{\beta}]. \quad (2.37)$$

If averages are obtained from KMC trajectories, $P_{\alpha} = s_{\alpha}/s$, where s_{α} is the number of Markov chains ending in the state α after time t , and s is the total number of chains.

Alternatively, one can calculate time averages by analyzing a single Markov chain. If the total occupation time of the state α is τ_{α} then

$$\bar{O} = \frac{1}{\tau} \sum_{\alpha} O_{\alpha} \tau_{\alpha}, \quad (2.38) \quad \text{equ:time}$$

where $\tau = \sum_{\alpha} \tau_{\alpha}$ is the total time used for time averaging.

For ergodic systems and sufficient sampling times, ensemble and time averages should give identical results. In many cases, the averaging procedure reflects a specific experimental technique. For example, an ensemble average over several KMC trajectories with different starting conditions corresponds to averaging over injected charge carriers in a time-of-flight experiment. In what follows, we focus on the single charge carrier (low concentration of charges) case.

2.11.1 Charge density

sec:occupation

For a specific type of particles, the microscopic charge density of a site i is proportional to the occupation probability of the site, p_i

$$\rho_i = e p_i / V_i, \quad (2.39)$$

where, for an irregular lattice, the effective volume V_i can be obtained from a Voronoi tessellation of space. For reasonably uniform lattices (uniform site densities) this volume is almost independent of the site and a constant volume per site, $V_i = V/N$, can be assumed. In the macroscopic limit, the charge density can be calculated using a sxtpting kernel function, i.e. a distance-weighted average over multiple sites. Site occupations p_i can be obtained from eq. (2.36) or eq. (2.38) by using the occupation of site i in state α as an observable.

If the system is in thermodynamic equilibrium, that is without sources or sinks and without circular currents (and therefore no net flux) a condition, known as detailed balance, holds

$$p_j \omega_{ji} = p_i \omega_{ij}, \quad (2.40) \quad \text{equ:detailed_balance}$$

It can be used to test whether the system is ergodic or not by correlating $\log p_i$ and the site energy E_i . Indeed, if $\lambda_{ij} = \lambda_{ji}$ the ratios of forward and backward rates are determined solely by the energetic disorder, $\omega_{ji}/\omega_{ij} = \exp(-\Delta E_{ij}/k_B T)$ (see eq. (2.31)).

2.11.2 Current

873

sec:vaverage

874

875

If the position of the charge, \vec{r} , is an observable, the time evolution of its average $\langle \vec{r} \rangle$ is the total current in the system

$$\vec{J} = e \langle \vec{v} \rangle = e \frac{d \langle \vec{r} \rangle}{dt} = e \sum_{i,j} p_j \omega_{ji} (\vec{r}_i - \vec{r}_j). \quad (2.41) \quad \text{equ:current_def}$$

876

Symmetrizing this expression we obtain

$$\vec{J} = \frac{1}{2} e \sum_{i,j} (p_j \omega_{ji} - p_i \omega_{ij}) \vec{r}_{ij}, \quad (2.42) \quad \text{equ:current}$$

877

878

where $\vec{r}_{ij} = \vec{r}_i - \vec{r}_j$. Symmetrization ensures equal flux splitting between neighboring sites and absence of local average fluxes in equilibrium. It allows to define a local current through site i as

$$\vec{J}_i = \frac{1}{2} e \sum_j (p_j \omega_{ji} - p_i \omega_{ij}) \vec{r}_{ij}. \quad (2.43) \quad \text{equ:site_current}$$

879

880

A large value of the local current indicates that the site contributes considerably to the total current. A collection of such sites thus represents most favorable charge pathways [44].

2.11.3 Mobility and diffusion constant

881

sec:mobility

882

883

884

For a single particle, e.g. a charge or an exciton, a zero-field mobility can be determined by studying particle diffusion in the absence of external fields. Using the particle displacement squared, Δr_i^2 , as an observable we obtain

$$2dD_{\gamma\delta} = \frac{d \langle \Delta r_{i,\gamma} \Delta r_{i,\delta} \rangle}{dt} = \sum_{\substack{i,j \\ i \neq j}} p_j \omega_{ji} (\Delta r_{i,\gamma} \Delta r_{i,\delta} - \Delta r_{j,\gamma} \Delta r_{j,\delta}) = \sum_{\substack{i,j \\ i \neq j}} p_j \omega_{ji} (r_{i,\gamma} r_{i,\delta} - r_{j,\gamma} r_{j,\delta}). \quad (2.44) \quad \text{equ:diffusion}$$

885

886

Here \vec{r}_i is the coordinate of the site i , $D_{\gamma\delta}$ is the diffusion tensor, $\gamma, \delta = x, y, z$, and $d = 3$ is the system dimension. Using the Einstein relation,

$$D_{\gamma\delta} = k_B T \mu_{\gamma\delta}, \quad (2.45)$$

887

888

889

890

891

892

893

894

one can, in principle, obtain the zero-field mobility tensor $\mu_{\gamma\delta}$. Eq. (2.44), however, does not take into account the use of periodic boundary conditions when simulating charge dynamics. In this case, the simulated occupation probabilities can be compared to the solution of the Smoluchowski equation with periodic boundary conditions (see the supporting information for details).

Alternatively, one can directly analyze time-evolution of the KMC trajectory and obtain the diffusion tensor from a linear fit to the mean square displacement, $\overline{\Delta r_{i,\gamma} \Delta r_{i,\delta}} = 2dD_{\gamma\delta}t$.

The charge carrier mobility tensor, $\hat{\mu}$, for any value of the external field can be determined either from the average charge velocity defined in eq. (2.41)

$$\langle \vec{v} \rangle = \sum_{i,j} p_j \omega_{ji} (\vec{r}_i - \vec{r}_j) = \hat{\mu} \vec{F}, \quad (2.46)$$

895

896

897

898

899

or directly from the KMC trajectory. In the latter case the velocity is calculated from the unwrapped (if periodic boundary conditions are used) charge displacement vector divided by the total simulation time. Projecting this velocity on the direction of the field \vec{F} yields the charge carrier mobility in this particular direction. In order to improve statistics, mobilities can be averaged over several KMC trajectories and MD snapshots.

2.11.4 Spatial correlations of energetic disorder

900

sec:eanalyze

901 Long-range, e.g. electrostatic and polarization, interactions often result in spatially correlated
902 disorder [45], which affects the onset of the mobility-field (Poole-Frenkel) dependence [40, 46, 47].

903 To quantify the degree of correlation, one can calculate the spatial correlation function of E_i and

904 E_j at a distance r_{ij}

$$C(r_{ij}) = \frac{\langle (E_i - \langle E \rangle) (E_j - \langle E \rangle) \rangle}{\langle (E_i - \langle E \rangle)^2 \rangle}, \quad (2.47) \text{ equ:cf}$$

905 where $\langle E \rangle$ is the average site energy. $C(r_{ij})$ is zero if E_i and E_j are uncorrelated and 1 if they are
906 fully correlated. For a system of randomly oriented point dipoles, the correlation function decays
907 as $1/r$ at large distances [48].

908 For systems with spatial correlations, variations in site energy differences, ΔE_{ij} , of pairs of
909 molecules from the neighbor list are smaller than variations in site energies, E_i , of all individ-
910 ual molecules. Since only neighbor list pairs affect transport, the distribution of ΔE_{ij} rather than
911 that of individual site energies, E_i , should be used to characterize energetic disorder.

912 Note that the `eanalyze` calculator takes into account *all* contributions to the site energies



Analyze distribution and correlations of site energies

```
| xtp_run -o options.xml -f state.sql -e eanalyze
```

913

914 Chapter 3

915 Input and output files

916 sec:io 3.1 Atomistic topology

sec:atomistic

917 If you are using GROMACS for generating atomistic configurations, it is possible to directly use
918 the topology file provided by GROMACS (`topology.tpr`). In this case the GROMACS residue and
919 atom names should be used to specify the coarse-grained topology and conjugated segments.
920 A custom topology can also be defined using an XML file. Moreover, it s possible to partially
921 overwrite the information provided in, for example, GROMACS topology file. We will illustrate
922 how to create a custom topology file using DCV2T. The structure of DCV2T, together with atom
923 type definitions, is shown in fig. 3.1. DCV2T has two thiophene (THI) and two dicyanovinyl
924 (NIT) residues. The pdb file which contains residue types, residue numbering, atom names,
925 atom types, and atom coordinates is shown in listing 3.1.

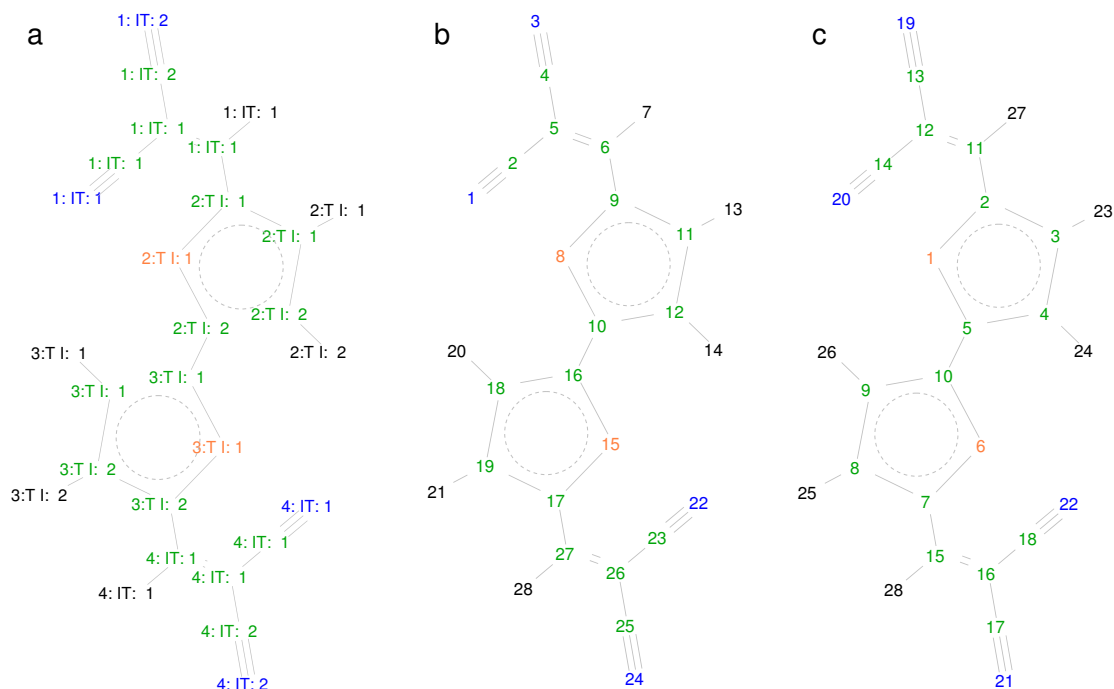


Figure 3.1: (a) DCV2T with atoms labelled according to `residue_number:residue_name:atom_name`. There are four residues and two residue types: thiophene (THI) and dicyanovinyl (NIT). The corresponding pdb file is shown in listing 3.1. Atom numbering is used to split conjugated segments on rigid fragments and to link atomistic (b) from GROMACS topology and quantum descriptions (c).

fig:dcv2t

list.pdb

Listing 3.1: pdb file of DCV2T.

926											
927	HETATM	1	N1	NIT	1	2.388	8.533	11.066	1.00	4.14	N
928	HETATM	2	CN1	NIT	1	1.984	9.553	10.718	1.00	2.54	C
929	HETATM	3	N2	NIT	1	-1.138	10.872	10.087	1.00	3.24	N
930	HETATM	4	CN2	NIT	1	0.003	10.871	10.213	1.00	2.37	C
931	HETATM	5	CC1	NIT	1	1.441	10.824	10.327	1.00	1.91	C
932	HETATM	6	C1	NIT	1	2.193	11.939	10.071	1.00	1.61	C
933	HETATM	7	HN1	NIT	1	1.715	12.710	9.872	1.00	1.97	H
934	HETATM	8	S1	THI	2	4.758	10.743	10.130	1.00	1.52	S
935	HETATM	9	CA1	THI	2	3.613	12.024	9.948	1.00	1.22	C
936	HETATM	10	CA2	THI	2	6.099	11.836	9.997	1.00	1.30	C
937	HETATM	11	CB1	THI	2	4.251	13.243	9.782	1.00	1.39	C
938	HETATM	12	CB2	THI	2	5.658	13.131	9.818	1.00	1.45	C
939	HETATM	13	HC1	THI	2	3.800	14.047	9.660	1.00	1.66	H
940	HETATM	14	HC2	THI	2	6.230	13.860	9.731	1.00	1.74	H
941	HETATM	15	S1	THI	3	8.803	12.414	9.882	1.00	1.38	S
942	HETATM	16	CA1	THI	3	7.456	11.347	10.094	1.00	1.37	C
943	HETATM	17	CA2	THI	3	9.940	11.122	10.152	1.00	1.42	C
944	HETATM	18	CB1	THI	3	7.873	10.048	10.355	1.00	1.73	C
945	HETATM	19	CB2	THI	3	9.267	9.926	10.399	1.00	1.82	C
946	HETATM	20	HC1	THI	3	7.288	9.335	10.487	1.00	2.05	H
947	HETATM	21	HC2	THI	3	9.704	9.123	10.576	1.00	2.21	H
948	HETATM	22	N1	NIT	4	11.235	14.572	9.094	1.00	3.08	N
949	HETATM	23	CN1	NIT	4	11.665	13.566	9.441	1.00	2.04	C
950	HETATM	24	N2	NIT	4	14.733	12.005	10.009	1.00	2.17	N
951	HETATM	25	CN2	NIT	4	13.590	12.149	9.933	1.00	1.77	C
952	HETATM	26	CC1	NIT	4	12.156	12.282	9.861	1.00	1.71	C
953	HETATM	27	C1	NIT	4	11.363	11.220	10.154	1.00	1.59	C
954	HETATM	28	HN1	NIT	4	11.813	10.440	10.389	1.00	1.89	H

tab:map

Table 3.1: Description of the XML mapping file (`map.xml`).

topology	Definitions of molecules, segments, and fragments.
molecules	Container for all molecules.
molecule	Mapping of a single molecule.
name	Name of the molecule in the coarse-grained model.
ident	Name (identification) of the molecule in the all-atom representation. This must match the molecule name in the atomistic representation.
segments	Partitioning of the molecule on conjugated segments.
segment	Description of a conjugated segment.
name	Name of a conjugated segment in a molecule.
fragments	Container for all fragments in a segment.
fragment	Description of a rigid fragment.
name	Name of the rigid fragment in a conjugated segment
mdatoms	List of all atoms belonging to the rigid fragment in the format residue number:residue name:atom name.
qmatoms	List of atoms of the rigid fragment in its ground state geometry, atom number:atom type.
weights	Weights are used to determine the fragment center. The order should be the same as in the mdatoms and qmatoms definitions. If the mass of a nucleus in atomic mass units is used, the center of the rigid fragment will be its center of mass.
localframe	Three atoms which define a local frame for each rigid fragment.

3.2 Mapping file

956

sec:xmlmap

The mapping file (referred here as `map.xml`) is used by the program `xtp_map` to convert an atomistic trajectory to a trajectory with conjugated segments and rigid fragments. This trajectory is stored in a state file and contains positions, names, types of atoms belonging to rigid fragments. The description of the mapping options is given in table 3.1. An example of `map.xml` for a DCV2T molecule is shown in listing 3.2.

The file `map.xml` contains the whole electrostatic information about the molecules as well as the structural information. The `toolpdb2map` creates a `map.xml` from a `pdb` file and is a good starting point for further refinement.

list:map

Listing 3.2: Examl of `map.xml` for DCV2T. Each rigid fragment (coarse-grained bead) is defined by a list of atoms. Atom numbers, names, and residue names should correspond to those used in GROMACS topology (see the corresponding listing 3.1 of the `pdb` file).

```

965 <!-- this file is used to conver an atomistic trajectory to conjugated segments -->
966 <!-- molecules -->
967 <!-- molecule -->
968 <!-- name of the conjugated molecule -->
969 <!-- corresponding name of this molecule in the MD trajectory, should be
970 the same as the name given at the end of topol.top -->
971 <!-- segments -->
972 <!-- segment -->
973 <!-- name of the conjugated segment within the molecule -->
974 <!-- QM coordinates of the conjugated segment -->
975 <!-- IZINDO INPUT -->
976 <!-- basisset -->
977 <!-- orbitals -->
978 <!-- Number of the HOMO Orbital (e.g. alpha electrons, can be
979 found in the log-file belonging to DCV2T.orb) -->
980 <!-- EMULTIPOLE INPUT -->
981 <!-- Multipole file for neutral state -->
982 <!-- Multipole file for hole state -->
983 <!-- specifies if planar QM coordinates (map2md=0) or MD coordinates (
984 map2md=1) of atoms are used for distribution of partial charges. For MD coordinates the
985 order and numbering in <!-- mdatoms --> and <!-- mpoles --> must be identical it has no impact on the
986 qm e.g. DFT or GWBSE calculations -->
987 <!-- EINTERNAL INPUT -->
988 <!-- Site energy -->

```

```

993 <U_nC_nN_h>0.1</U_nC_nN_h> <!-- Reorg. discharge -->
994 <U_nC_nC_h>0.1</U_nC_nC_h> <!-- Reorg. charge -->
995
996 <!-- MD QM MP Mapping -->
997 <fragments>
998 <fragment>
999 <name>N1</name> <!-- name of the rigid fragment within the segment -->
1000 <!-- list of atoms in the fragment resnum:resname:atomname -->
1001 <mdatoms>1:NIT:N1 1:NIT:CN1 1:NIT:N2 1:NIT:CN2 1:NIT:CC1 1:NIT:C1 1:NIT:HN1</mdatoms>
1002 <!-- corresponding ground state geometry atomnumber:atomtype read from .xyz file-->
1003 <qmatoms> 20:N 19:C 14:N 13:C 12:C 11:C 23:H </qmatoms>
1004 <!-- corresponding group state geometry multipoles read from .mps files -->
1005 <mpoles> 20:N 19:C 14:N 13:C 12:C 11:C 23:H </mpoles>
1006 <!-- weights to determine the fragment center (here CoM is used) -->
1007 <weights> 14 12 14 12 12 12 1 </weights>
1008 <!-- three atoms: define a cartesian local frame, two atoms: fragment is assumed to be
1009 rotationally invariant around the axis, one atom: fragment is assumed isotropic -->
1010 <localframe> 20 19 14 </localframe>
1011 <!-- Optional parameters (if not set <localframe> is used): used when atom labels in the .mps
1012 and .xyz file differ or more sites in the .mps file are used, so refers to <mpoles> -->
1013 <localframe_mps> 20 19 14 </localframe_mps>
1014 <!-- Optional parameters (if not set <localframe> is used): weights to determine the
1015 fragment center (here CoM is used), used when atom labels in the .mps and .xyz file
1016 differ or additional sites in the .mps file are used -->
1017 <weights_mps> 14 12 14 12 12 12 1 </
1018 weights_mps>
1019 <!-- Optional flag: says if a site is virtual or not, (virtual=1, real=0)-->
1020 <virtual_mps> 0 0 0 0 0 0 0 </
1021 virtual_mps>
1022 </fragment>
1023
1024 <fragment>
1025 <name>TH1</name>
1026 <mdatoms>2:THI:S1 2:THI:CA1 2:THI:CA2 2:THI:CB1 2:THI:CB2 2:THI:HC1 2:THI:HC2</mdatoms>
1027 <qmatoms> 7:S 8:C 6:C 9:C 10:C 24:H 25:H </qmatoms>
1028 <mpoles> 7:S 8:C 6:C 9:C 10:C 24:H 25:H </mpoles>
1029 <weights> 32 12 12 12 12 1 1 </weights>
1030 <localframe> 7 8 6 </localframe>
1031 </fragment>
1032
1033 <fragment>
1034 <name>TH2</name>
1035 <mdatoms>3:THI:CA1 3:THI:CA2 3:THI:CB1 3:THI:CB2 3:THI:HC1 3:THI:HC2</mdatoms>
1036 <qmatoms> 3:S 4:C 2:C 5:C 1:C 26:H 27:H </qmatoms>
1037 <weights> 32 12 12 12 12 1 1 </weights>
1038 <localframe> 3 4 2 </localframe>
1039 </fragment>
1040
1041 <fragment>
1042 <name>N12</name>
1043 <mdatoms>4:NIT:N1 4:NIT:CN1 4:NIT:N2 4:NIT:CN2 4:NIT:CC1 4:NIT:C1 4:NIT:HN1</mdatoms>
1044 <qmatoms> 22:N 21:C 18:N 17:C 16:C 15:C 28:H </qmatoms>
1045 <mpoles> 22:N 21:C 18:N 17:C 16:C 15:C 28:H </mpoles>
1046 <weights> 14 12 14 12 12 12 1 </weights>
1047 <localframe> 22 21 18 </localframe>
1048 </fragment>
1049 </fragments>
1050 </segment>
1051 </segments>
1052 </molecule>
1053 </molecules>
1054 </topology>

```

3.3 Molecular orbitals

1056 If the semi-empirical method is used to calculate electronic coupling elements, molecular or-
1057 bitals of all molecules must be supplied. They can be generated using Gaussian program. The
1058 Gaussian input file for DCV2T is shown in listing 3.3. Provided with this input, Gaussian will
1059 generate fort. 7 file which contains the molecular orbitals of a DCV2T. This file can be renamed
1060 to DCV2T.orb. Note that the order of the atoms in the input file and the order of coefficients
1061 should always match. Therefore, the coordinate part of the input file must be supplied together
1062 with the orbitals. We will assume the coordinates, in the format atom_type: x y z, is saved
1063 to the DCV2T.xyz file.
1064

⚠ Be careful!

Izindo requires the specification of orbitals for hole and electron transport in `map.xml`. They are the HOMO and LUMO respectively and can be retrieved from the `log` file from which the `DCV2T.orb` file is generated. The number of alpha electrons is the HOMO, the LUMO is HOMO+1

1065

list:zindo_orbitals

Listing 3.3: Gaussian input file `get_orbitals.com` used for generating molecular orbitals. The first line contains the name of the check file, the second the requested RAM. `int=zindos` requests the method ZINDO, `punch=mo` states that the molecular orbitals ought to be written to the `fort.7` file, `nosymm` forbids use of symmetry and is necessary to ensure correct position of orbitals with respect to the provided coordinates. The two integer numbers correspond to the charge and multiplicity of the system: 0 1 corresponds to a neutral system with a multiplicity of one. They are followed by the types and coordinates of all atoms in the molecule.

```

1066 %chk=DCV2T.chk
1067 %mem=100Mb
1068
1069 #p int=zindos punch=mo nosymm
1070
1071 DCV2T molecular orbitals
1072
1073 0 1
1074 S      -1.44650      2.12185      0.00135
1075 C      -2.43098      0.58936     -0.00048
1076 C      -1.59065     -0.51859     -0.00146
1077 C      -0.21222     -0.22233     -0.00095
1078 C       0.07761      1.13376      0.00040
1079 S       2.87651      0.79316      0.00148
1080 C       3.86099      2.32565      0.00235
1081 C       3.02066      3.43359      0.00231
1082 C       1.64223      3.13733      0.00162
1083 C       1.35240      1.78125      0.00114
1084 C      -3.85350      0.52245     -0.00081
1085 C      -4.79569      1.52479     -0.00008
1086 C      -6.18500      1.18622     -0.00117
1087 C      -4.47544      2.91565      0.00081
1088 C       5.28350      2.39256      0.00296
1089 C       6.22569      1.39020      0.00327
1090 C       7.61500      1.72876      0.00432
1091 C       5.90542     -0.00064      0.00333
1092 N      -7.32389      0.89743     -0.00195
1093 N      -4.21872      4.06274      0.00142
1094 N       8.75389      2.01754      0.00510
1095 N       5.64864     -1.14772      0.00361
1096 H      -1.98064     -1.52966     -0.00256
1097 H       0.55785     -0.98374     -0.00169
1098 H       3.41065      4.44466      0.00272
1099 H       0.87216      3.89874      0.00147
1100 H      -4.24640     -0.49192     -0.00188
1101 H       5.67641      3.40692      0.00337

```

1103 3.4 Monomer calculations for DFT transfer integrals

list:edft_gaussian_xml

Listing 3.4: Example `package.xml` file for the Gaussian package required in the options of the `edft calculator` for the monomer calculations as preparation for the determination of transfer integrals using DIPRO.

```

1104 <package>
1105   <name>gaussian</name>
1106   <executable>g09</executable>
1107   <checkpoint></checkpoint>
1108   <scratch></scratch>
1109

```

```

1110 <charge>0</charge>
1111 <spin>1</spin>
1112 <options># pop=minimal pbepbe/6-311g** scf=tight punch=mo nosymm test</options>
1113 <memory>1Gb</memory>
1114 <threads>2</threads>
1115
1116
1117 <cleanup></cleanup>
1118 </package>

```

list.edft_turbomole.xml

Listing 3.5: Example `package.xml` file for the Turbomole package required in the options of the `edft calculator` for the monomer calculations as preparation for the determination of transfer integrals using DIPRO.

```

1120 <package>
1121 <name>turbomole</name>
1122 <executable>ridft</executable>
1123 <scratch>/tmp</scratch>
1124
1125 <options>
1126 TITLE
1127 a coord
1128 *
1129 no
1130 b all def-TZVP
1131 *
1132 eht
1133 y
1134 0
1135 y
1136 dft
1137 on
1138 func
1139 pbe
1140 grid
1141 m3
1142 *
1143 ri
1144 on
1145 m 300
1146 *
1147 scf
1148 conv
1149 7
1150 iter
1151 200
1152 marij
1153 q
1154 </options>
1155
1156 <cleanup></cleanup>
1157 </package>

```

list.edft_nwchem.xml

Listing 3.6: Example `package.xml` file for the NWChem package required in the options of the `edft calculator` for the monomer calculations as preparation for the determination of transfer integrals using DIPRO.

1162

```

1163 <package>
1164   <name>nwchem</name>
1165   <executable>nwchem</executable>
1166   <checkpoint></checkpoint>
1167   <scratch>/tmp/nwchem</scratch>
1168   <charge>0</charge>
1169   <spin>1</spin>
1170   <threads>1</threads>
1171   <memory></memory>
1172   <options>
1173     start
1174     basis
1175     * library 6-311gss
1176     end
1177     memory 1500 mb
1178
1179     dft
1180     xc xpbe96 cpbe96
1181     direct
1182     iterations 100
1183     noprint "final vectors analysis"
1184     end
1185     task dft
1186   </options>
1187   <cleanup></cleanup>
1188 </package>

```

3.5 Pair calculations for DFT transfer integrals

list:ldft_gaussian_xml

Listing 3.7: Example `package.xml` file for the Gaussian package required in the options of the `ldft` calculator for the pair calculations and the determination of transfer integrals using DIPRO.

```

1191 <package>
1192   <name>gaussian</name>
1193   <executable>g09</executable>
1194   <checkpoint></checkpoint>
1195   <scratch></scratch>
1196
1197   <charge>0</charge>
1198   <spin>1</spin>
1199   <options># pop=minimal pbepbe/6-311g** nosymm IOp(3/33=1,3/36=-1) punch=mo guess=cards scf=
1200   <memory>1Gb</memory>
1201   <threads>1</threads>
1202
1203   <cleanup></cleanup>
1204 </package>
1205
1206

```

list:ldft_turbomole_xml

Listing 3.8: Example `package.xml` file for the Turbomole package required in the options of the `ldft` calculator for the pair calculations and the determination of transfer integrals using DIPRO.

```

1207 <package>
1208   <name>turbomole</name>
1209   <executable>ridft</executable>
1210   <scratch>/tmp</scratch>
1211
1212   <options>
1213     $intsdebug cao
1214

```

```

1215 a coord
1216 *
1217 no
1218 b all def-TZVP
1219 *
1220 eht
1221 y
1222 0
1223 y
1224 dft
1225 on
1226 func
1227 pbe
1228 grid
1229 m3
1230 *
1231 ri
1232 on
1233 m 300
1234 *
1235 scf
1236 conv
1237 7
1238 iter
1239 1
1240 diis
1241 3
1242 damp
1243 0.00
1244
1245
1246
1247 marij
1248
1249 q
1250 </options>
1251
1252 <cleanup></cleanup>
1253 </package>
1254

```

list:ldft_nwchem.xml

Listing 3.9: Example `package.xml` file for the NWChem package required in the options of the `ldft` calculator for the pair calculations and the determination of transfer integrals using `DIPRO`.

```

1255 <package>
1256 <name>nwchem</name>
1257 <executable>nwchem</executable>
1258 <checkpoint></checkpoint>
1259 <scratch>/tmp/nwchem</scratch>
1260 <charge>0</charge>
1261 <spin>1</spin>
1262 <memory></memory>
1263 <threads>1</threads>
1264 <options>
1265 start
1266 basis
1267 * library 6-311gss
1268 end
1269 memory 1500 mb
1270
1271

```

```

1272 dft
1273   print "ao overlap"
1274   xc xpbe96 cpbe96
1275   direct
1276   iterations 1
1277   convergence nodamping nodiis
1278   noprint "final vectors analysis"
1279   vectors input system.movecs
1280 end
1281 task dft
1282 </options>
1283   <cleanup></cleanup>
1284 </package>

```

3.6 DFT transfer integrals

list:TI.xml

Listing 3.10: Example TI.xml file created as the output of a DIPRO calculation. Due to slightly different implementations, the orbitals indices refer to monomer indices in a Gaussian run but to indices in the merged dimer guess in a Turbomole run.

```

1287 <pair name="pair_100_155">
1288   <parameters>
1289     <HOMO_A>162</HOMO_A>
1290     <NoccA>1</NoccA>
1291     <LUMO_A>164</LUMO_A>
1292     <NvirtA>1</NvirtA>
1293     <HOMO_B>161</HOMO_B>
1294     <NoccB>1</NoccB>
1295     <LUMO_B>163</LUMO_B>
1296     <NvirtB>1</NvirtB>
1297   </parameters>
1298   <transport name="hole">
1299     <channel name="single">
1300       <J>1.546400416750696E-003</J>
1301       <e_A>-6.30726450715697</e_A>
1302       <e_B>-6.36775613794166</e_B>
1303     </channel>
1304     <channel name="multi">
1305       <molecule name="A">
1306         <e_HOMOm0>-6.30726450715697</e_HOMOm0>
1307       </molecule>
1308       <molecule name="B">
1309         <e_HOMOm0>-6.36775613794166</e_HOMOm0>
1310       </molecule>
1311       <dimer name="integrals">
1312         <T_00>1.546400416750696E-003</T_00>
1313         <J_sq_degen>2.391354248926727E-006</J_sq_degen>
1314         <J_sq_boltz>2.391354248926727E-006</J_sq_boltz>
1315       </dimer>
1316     </channel>
1317   </transport>
1318   <transport name="electron">
1319     <channel name="single">
1320       <J>-2.797473760331286E-003</J>
1321       <e_A>-4.50318366770689</e_A>
1322       <e_B>-4.53143397059021</e_B>
1323     </channel>
1324

```

```

1325     <channel name="multi">
1326         <molecule name="A">
1327             <e_LUMOp0>-4.50318366770689</e_LUMOp0>
1328         </molecule>
1329         <molecule name="B">
1330             <e_LUMOp0>-4.53143397059021</e_LUMOp0>
1331         </molecule>
1332         <dimer name="integrals">
1333             <T_00>-2.797473760331286E-003</T_00>
1334             <J_sq_degen>7.825859439742066E-006</J_sq_degen>
1335             <J_sq_boltz>7.825859439742066E-006</J_sq_boltz>
1336         </dimer>
1337     </channel>
1338 </transport>
1339 </pair>

```

1341 3.7 State file

sec:statefile

1342 All data structures are saved to the `state.sql` file in `sqlite3` format, see <http://www.sqlite.org/>.

1343 They are available in form of tables in the `state.sql` file as can be seen by the command

1344 `sqlite3 state.sql ".tables "`

1345 An example of such a table are `molecules`. The full table can be displayed using the command

1346 (similar for the other tables)

1347 `sqlite3 state.sql " SELECT * FROM molecules "`

1348 The meaning of all the entries in the table can be displayed by a command like

1349 `sqlite3 state.sql ".SCHEMA molecules "`

1350 The first and second entry are integers for internal and regular id of the molecule and the third

1351 entry is the name. A single field from the table like the name of the molecule can be displayed by

1352 a command like

1353 `sqlite3 state.sql " SELECT name FROM molecules "`

1354 Besides `molecules`, the following tables are stored in the `state.sql`:

1355 `conjseg_properties`:

1356 Conjugated segments are stored with id, name and x,y,z coordinates of the center of mass in nm.

1357 `conjsegs`:

1358 Reorganization energies for charging or discharging a conjugated segment are stored together

1359 with the coulomb energy and any other user defined energy contribution (in eV) and occupation

1360 probabilities.

1361 `pairs`:

1362 The pairs from the neighborlist are stored with the pair id, the id of the first and second segment,

1363 the rate from the first to the second , the rate from the second to the first (both in s^{-1}) and the

1364 x,y,z coordinates in nm of the distance between the first and the second segment.

1365 `pairintegrals`:

1366 Transfer integrals for all pairs are stored in the following way: The pair id , the number for counting

1367 possible different electronic overlaps (e.g if only the frontier orbitals are taken into account

1368 this is always zero, while an effective value is stored in addition to the different overlaps of e.g.

1369 HOMO-1 and HOMO-1 if more frontier orbitals are taken into account) and the integral in eV.

1370 `pairproperties`:

1371 The outer sphere reorganization energy of all pairs is stored by an id, the pair id, a string `lambda_outer`

1372 and the energy in eV.

1373 `conjsegs`:

1374 Conjugated segments are saved in the following way: The id, the name, the type, the molecule

1375 id, the time frame, the x,y,z coordinates in nm and the occupation probability.

1376 `conjseg_properties`:

1377 Properties of the conjugated segments like reorganization energies for charging or discharging a
 1378 charge unit or the coulomb contribution to the site energy are stored by: id, conjugated segment
 1379 id, a string like `lambda_intra_charging`, `lambda_intra_discharging` or `energy_coulomb`
 1380 and a corresponding value in eV.

1381 The tables `rigidfrag_properties`, `rigidfrags` and `frames` offer information about rigid
 1382 fragments and time frames including periodic boundary conditions.

1383 The data in the `state.sql` file can also be modified by the user. Here is an example how to
 1384 modify the transfer integral between the conjugated segments number one and two assuming
 1385 that they are in the neighborlist. Their pair id can be found by the command

```
1386 pair_ID=`sqlite3 state.sql "SELECT _id FROM pairs WHERE conjseg1=1 AND conjseg2=2" `
```

1387 The old value of the transfer integral can be deleted using

```
1388 sqlite3 state.sql "DELETE FROM pair_integrals WHERE pair=$pair_ID"
```

1389 Finally the new transfer integral J can be written to the `state.sql` file by the command

```
1390 sqlite3 state.sql "INSERT INTO pair_integrals (pair,num,J) VALUES ($pair_ID,0,$J) "
```

1391 Here the `num=0` indicates that only the effective transfer integrals is written to the file, while other
 1392 values of `num` would correspond to overlap between other orbitals than the frontier orbitals.

1393 In a similar way the coulomb contribution to the site energy of the first conjugated segment can
 1394 be overwritten by first getting its id

```
1395 c_ID=`sqlite3 state.sql "SELECT _id from conjseg_properties where conjseg=1 AND
```

```
1396 key =\"energy_coulomb\""
```

1397 Then deleting the old value

```
1398 sqlite3 state.sql "DELETE FROM from conjseg_properties WHERE _id=$c_ID"
```

1399 Then the new coulomb energy E can be written to this id

```
1400 sqlite3 state.sql "INSERT INTO conjseg_properties (_id,conjseg,key,value)
```

```
1401 VALUES ($c_ID,1,\"energy_coulomb\",$E) "
```

1402 Finally the resulting coulomb contribution to all conjugated segments can be displayed by

```
1403 sqlite3 state.sql "SELECT * from conjseg_properties WHERE key=\"energy_coulomb\""
```

1404

1405 Chapter 4

1406 Reference

sec:reference

1407 4.1 Programs

sec:programs

1408 Programs execute specific tasks (calculators).

1409 4.1.1 xtp_testsuite

prog:xtp_testsuite

1410 Performs tests en suite + optional arguments:

```
1411     -h, --help show this help message and exit
1412     -e [ [ ...]], --execute [ [ ...]] Tests to perform, accepts regex (def=".*")
1413     -l, --listonly List all tests available, then quit.
1414     -x , --xml Test-suite file (def="$VOTCASHARE/xtp/xml/testsuite.xml")
1415     -s , --source Test source input directory (def="source")
1416     -td , --testdirectory Test run directory (def="suite")
1417     -t , --target Directory where to store targets (def="targets")
1418     -r , --reference Folder with reference data to compare to (def="reference")
1419     -g, --generate Generate reference from targets (def=False)
1420     -cmp, --compareonly Only compare existing targets to reference (def=False)
1421     -v, --verbose The wordy version (def=False)
1422     -sh, --showoutput Display VOTCA::XTP exec. output (def=False)
1423     -c, --clean To clean or not to clean test dir. (def=False)
1424     -m , --mailto Mail the result. (def=False)
```

1425 4.1.2 xtp_update

prog:xtp_update

1426 Updates the state file + optional arguments:

```
1427     -h, --help show this help message and exit
1428     -f SQLFILE, --file SQLFILE State file to update.
```

1429 4.1.3 xtp_update_exciton

prog:xtp_update_exciton

1430 Updates the state file for singlets and triplets + optional arguments:

```
1431     -h, --help show this help message and exit
1432     -f SQLFILE, --file SQLFILE State file to update.
```

1433 4.1.4 xtp_basisset

prog:xtp_basisset

1434 xtp_update, version 1.4_rc1 Creates votca xml basissetfiles from NWCHEM basissetfiles optional
1435 arguments:

```

1436     -h, --help show this help message and exit
1437     -f NWCHEM, --inputnw NWCHEM NWchem file containing the basisset.
1438     -o OUTPUTFILE, --outputvotca OUTPUTFILE Path of votca outputfile

```

1439 4.1.5 xtp_map

prog:xtp_map

```

1440 Generates QM|MD topology
1441     -h [ --help ] display this help and exit
1442     -v [ --verbose ] be loud and noisy
1443     -t [ --topology ] arg topology
1444     -c [ --coordinates ] arg coordinates or trajectory
1445     -s [ --segments ] arg definition of segments and fragments
1446     -f [ --file ] arg state file

```

1447 4.1.6 xtp_run

prog:xtp_run

```

1448 Runs excitation/charge transport calculators
1449     -h [ --help ] display this help and exit
1450     -v [ --verbose ] be loud and noisy
1451     -o [ --options ] arg calculator options
1452     -f [ --file ] arg sqlight state file, *.sql
1453     -i [ --first-frame ] arg (=1) start from this frame
1454     -n [ --nframes ] arg (=1) number of frames to process
1455     -t [ --nthreads ] arg (=1) number of threads to create
1456     -s [ --save ] arg (=1) whether or not to save changes to state file
1457     -e [ --execute ] arg List of calculators separated by ',' or ''
1458     -l [ --list ] Lists all available calculators
1459     -d [ --description ] arg Short description of a calculator

```

1460 4.1.7 xtp_tools

prog:xtp_tools

```

1461 Runs excitation/charge transport tools
1462     -h [ --help ] display this help and exit
1463     -v [ --verbose ] be loud and noisy
1464     -t [ --nthreads ] arg (=1) number of threads to create
1465     -o [ --options ] arg calculator options Tools:
1466     -e [ --execute ] arg List of tools separated by ',' or ''
1467     -l [ --list ] Lists all available tools
1468     -d [ --description ] arg Short description of a tool

```

1469 4.1.8 xtp_parallel

prog:xtp_parallel

```

1470 Runs job-based heavy-duty calculators
1471     -h [ --help ] display this help and exit
1472     -v [ --verbose ] be loud and noisy
1473     -o [ --options ] arg calculator options
1474     -f [ --file ] arg sqlite state file, *.sql
1475     -i [ --first-frame ] arg (=1) start from this frame
1476     -n [ --nframes ] arg (=1) number of frames to process
1477     -t [ --nthreads ] arg (=1) number of threads to create
1478     -s [ --save ] arg (=1) whether or not to save changes to state file
1479     -r [ --restart ] arg restart pattern: 'host(pc1:234) stat(FAILED)'
1480     -c [ --cache ] arg (=8) assigns jobs in blocks of this size
1481     -j [ --jobs ] arg (=run) task(s) to perform: input, run, import

```

```

1482     -m [ --maxjobs ] arg (=-1) maximum number of jobs to process (-1 = inf)
1483     -e [ --execute ] arg List of calculators separated by ',' or ''
1484     -l [ --list ] Lists all available calculators
1485     -d [ --description ] arg Short description of a calculator

```

1486 4.1.9 xtp_dump

prog:xtp_dump

```

1487 Extracts information from the state file
1488     -h [ --help ] display this help and exit
1489     -v [ --verbose ] be loud and noisy
1490     -o [ --options ] arg calculator options
1491     -f [ --file ] arg sqlight state file, *.sql
1492     -i [ --first-frame ] arg (=1) start from this frame
1493     -n [ --nframes ] arg (=1) number of frames to process
1494     -t [ --nthreads ] arg (=1) number of threads to create
1495     -s [ --save ] arg (=1) whether or not to save changes to state file Extractors:
1496     -e [ --extract ] arg List of extractors separated by ',' or ''
1497     -l [ --list ] Lists all available extractors
1498     -d [ --description ] arg Short description of an extractor

```

1499 4.1.10 xtp_overlap

prog:xtp_overlap

```

1500 moo_overlap
1501     -h [ --help ] display this help and exit
1502     -v [ --verbose ] be loud and noisy MOO Options:
1503     --conjseg arg xml file describing two conjugated segments
1504     --pos1 arg position and orientation of molecule 1
1505     --pos2 arg position and orientation of molecule 2
1506     --pdb arg (=geometry.pdb) pdb file of two molecules

```

1507 4.1.11 xtp_kmc_run

prog:xtp_kmc_run

```

1508 kmc_run, version 1.4_rc1 (compiled Sep 26 2016, 22:47:52) Runs specified calculators
1509     -h [ --help ] display this help and exit
1510     -v [ --verbose ] be loud and noisy
1511     -o [ --options ] arg program and calculator options
1512     -f [ --file ] arg sqlite state file
1513     -t [ --textfile ] arg output text file (otherwise: screen output)
1514     -e [ --execute ] arg list of calculators separated by commas or spaces
1515     -l [ --list ] lists all available calculators
1516     -d [ --description ] arg detailed description of a calculator

```

1517 4.2 Calculators

sed:calculators

1518 Calculator is a piece of code which computes specific system properties, such as site energies,
 1519 transfer integrals, etc. `xtp_run`, `xtp_kmc_run` are wrapper programs which executes such
 1520 calculators. The generic syntax is

```
1521 xtp_run -e "calc1, calc2, ..." -o options.xml
```

1522 File `options.xml` lists all options needed to run a specific calculator. The format of this file is
 1523 explained in listing 4.1. A complete list of calculators is given in the `calculators` reference section.

list:calc

Listing 4.1: A part of the `options.xml` file with options for the `calculator_name{1,2}` calculators.

```

1524
1525 <calculator_name1>
1526     <option1>value1</option1>
1527     <option2>value2</option2>
1528     ...
1529 </calculator_name1>
1530
1531 <calculator_name2>
1532     <option1>value1</option1>
1533     <option2>value2</option2>
1534     ...
1535 </calculator_name2>
1536 ...
1537

```

A list of all calculators and their short descriptions can be obtain using

```
xtp_run --list
```

A detailed description of all options of a specific calculator(s) is available via

```
xtp_run --desc calc1,calc2,...
```

4.2.1 coupling

calc:coupling

Electronic couplings from log and orbital files (GAUSSAIN, TURBOMOLE, NWChem)

1543

option	default	unit	description
dftpackage			First-principles package
output	coupling.out.xml		Output file
degeneracy	0	eV	Criterion for the degeneracy of two levels
moleculeA			
log	A.log		Log file of molecule A
orbitals	A.orb		Orbitals file
levels	3		Output HOMO, ..., HOMO-levels; LUMO, ..., LUMO+levels
trim	2		
moleculeB			
log	B.log		Log file of molecule B
orbitals	B.orb		Orbitals file
levels	3		Output HOMO, ..., HOMO-levels; LUMO, ..., LUMO+levels
trim	2		
dimerAB			
log	AB.log		Log file of dimer AB
orbitals	A.orb		Orbitals file

Return to the description of `coupling`.

4.2.2 excitoncoupling

calc:excitoncoupling

Exciton couplings from serialized orbital files

1546

option	default	unit	description
classical			
output	excitoncoupling		Output file
bsecoupling_options			
orbitalsA	A.orb		Serialized orbitals file
orbitalsB	B.orb		Serialized orbitals file
orbitalsAB	AB.orb		Serialized orbitals file

1547 Return to the description of `excitoncoupling`.

1548 4.2.3 `gencube`

calc:gencube

1549 Tool to generate cube files from `.orb` file

option	default	unit	description
output	state.cube		Output file
input	system.orb		Input file
padding	6.5		How far the grid should start from the molecule
xsteps	25		Gridpoints in x-direction
ysteps	25		Gridpoints in y-direction
zsteps	25		Gridpoints in z-direction
state	1		State to generate cube file for
spin			Singlet or Triplet
type	ground		qp:quasiparticle,ground:groundstate,transition:transitionstate,excited/excitedstate density/density excited-ground state
mode	new		new: generate new cube file, subtract: subtract to cube files specified below
infile1			Cubefile to subtract infile2 from
infile2			Cubefile to subtract from infile1

1550 Return to the description of `gencube`.

1551 4.2.4 `log2mps`

calc:log2mps

1552 Generates an mps-file (with polar-site definitions) from a QM log-file

option	default	unit	description
package			QM package
logfile			Log-file generated by QM package, with population/esp-fit data

1553 Return to the description of `log2mps`.

1554 4.2.5 `molpol`

calc:molpol

1555 Molecular polarizability calculator (and optimizer)

option	default	unit	description
mpsfiles			
input			mps input file
output			mps output file
polar			xml file with infos on polarizability tensor
induction			
expdamp			Thole sharpness parameter
wSOR			mixing factor for convergence
maxiter			maximum number of iterations
tolerance			rel. tolerance for induced moments
target			
optimize			if 'true', refine atomic polarizabilities to match molecular polarizable volume specified in target.molpol
molpol			target polarizability tensor in format xx xy xz yy yz zz (this should be in the eigen-frame, hence xy = xz = yz = 0), if optimize=true the associated polarizable volume will be matched iteratively and the resulting set of polar sites written to mpsfiles.output

tolerance			relative tolerance when optimizing the polarizable volume
-----------	--	--	---

1556 Return to the description of `molpol`.

1557 4.2.6 orb2isogwa

1558 `calc:orb2isogwa` Analysis tool for QM results stores in serialized file

option	default	unit	description
output	qmanalyze.out		Output file
property			
input	molecule.orb		Serialized file

1559 Return to the description of `orb2isogwa`.

1560 4.2.7 partialcharges

1561 `calc:partialcharges` Tool to derive partial charges from QM results stores in serialized file

option	default	unit	description
output	Moleculecharge		Output file either .mps or .pdb
input	molecule.orb		Serialized file
esp_options			options for the method

1562 Return to the description of `partialcharges`.

1563 4.2.8 pdb2map

1564 `calc:pdb2map` Converts MD + QM files to VOTCA mapping. Combinations: `pdb+xyz,gro+xyz,pdb`

option	default	unit	description
pdb	conf.pdb		Input pdb file
gro	conf.gro		Input gro file
xyz	conf.xyz		Input xyz file
xml	conf.xml		Resulting xml file

1565 Return to the description of `pdb2map`.

1566 4.2.9 pdb2top

1567 `calc:pdb2top` Generates fake Gromacs topology file .top

option	default	unit	description
num	1		Num of mols in the box
pdb	conf.pdb		Input pdb file
gro	conf.gro		Input gro file

1568 Return to the description of `pdb2top`.

1569 4.2.10 ptopreader

1570 `calc:ptopreader` Reads binary .ptop-files (serialized from `ewdbgpol`) and processes them into something readable

option	default	unit	description
ptop_file			Binary archive .ptop-file

1571 Return to the description of `ptopreader`.

1572 4.2.11 `qmanalyze`

1573 `calc:qmanalyze` Analysis tool for QM results stores in serialized file

option	default	unit	description
output	qmanalyze.out		Output file
BSE			additional info about BSE results
input	molecule.orb		Serialized file

1574 Return to the description of `qmanalyze`.

1575 4.2.12 `eanalyze`

1576 `calc:eanalyze` Histogram and correlation function of site energies and pair energy differences

option	default	unit	description
resolution_sites		eV	Bin size for site energy histogram
resolution_pairs		eV	Bin size for pair energy histogram
resolution_space		eV	Bin size for site energy correlation
states			?

1577 Return to the description of `eanalyze`.

1578 4.2.13 `eimport`

1579 `calc:eimport` Imports site energies from the output file of `emultipole` and writes them to the state file

option	default	unit	description
--------	---------	------	-------------

1580 Return to the description of `eimport`.

1581 4.2.14 `einternal`

1582 `calc:einternal` Reads in site and reorganosation energies and writes them to the state file

option	default	unit	description
energiesXML			XML input file with vacuum site, reorganization (charging, discharging) energies

1583 Return to the description of `einternal`.

1584 4.2.15 `emultipole`

1585 `calc:emultipole` Evaluates polarization contribution based on the Thole model

option	default	unit	description
multipoles			Polar Site Definitions in GDMA punch-file format
control			Control options for induction computation
induce	1		Enter '1' / '0' to toggle induction on / off
first			First segment for which to compute site energies
last			Last segment for which to compute site energies
output			File to write site energies to. Site energies are also stored in the state file
check			Check mapping of polar sites to fragment

tholeparam			Thole parameters required for charge-smearing
cutoff		nm	Cut-off beyond which all interactions are neglected
cutoff2		nm	Cut-off beyond which polarization is neglected
expdamp			Damping exponent used in exponential damping function
scaling			1-n interaction scaling, currently not in use
esp			Control options for potential calculation
calcESP			Enter '1' / '0' to toggle on / off. If '1', site energies will not be evaluated
cube			
grid			XYZ file specifying grid points for potential evaluation
output			File to write grid-point potential to
esf			Control options for field calculation
calcESF			Enter '1' / '0' to toggle on / off. If '1', site energies will not be evaluated
grid			XYZ file specifying grid points for field evaluation
output			File to write grid-point field to
alphamol			Control options for molecular-polarizability calculation
calcAlpha			Enter '1' / '0' to toggle on / off. If '1', site energies will not be evaluated
output			File to write polarizability tensor in global frame and in diagonal form to
convparam			Convergence parameters for self-consistent field calculation
wSOR_N			Mixing factor for successive overrelaxation of neutral system, usually between 0.3 and 0.5
wSOR_C			Mixing factor for successive overrelaxation of charged system, usually between 0.3 and 0.5
tolerance			Convergence criterion, fulfilled if relative change smaller than tolerance
maxiter			Maximum number of iterations in the convergence loop

1586 [Return to the description of `emultipole`.](#)

1587 4.2.16 `eoutersphere`

calc:eoutersphere

1588 Evaluates outersphere reorganization energy

option	default	unit	description
multipoles			XML allocation polar sites
method			Type of the method: <code>constant</code> - all pairs have value <code>lambda</code> . <code>spheres</code> - molecules are treated as spheres with radii <code>radius</code> and Pekar factor <code>pekar</code> . <code>dielectric</code> - with Pekar factor <code>pekar</code> and partial charges from resulting dielectric fields
lambdaconst		eV	The value for all pairs in the <code>constant</code> method
pekar			Pekar factor used for methods <code>spheres</code> and <code>dielectric</code>
segment			
type			
radius			
segment			
type			
radius			
cutoff		nm	Cutoff radius in between pair and the exterior molecule. Can be used in <code>spheres</code> and <code>dielectric</code>

1589 [Return to the description of `eoutersphere`.](#)

1590 **4.2.17 ianalyze**

1591 `calc:ianalyze` Evaluates a histogram of a logarithm of squared couplings

option	default	unit	description
resolution_logJ2			Bin size of histogram $\log(J^2)$
resolution_space		nm	Bin size for r in $\log(J^2(r))$
states			States for which to calculate the histogram. Example: 1 -1

1592 Return to the description of `ianalyze`.

1593 **4.2.18 iimport**

1594 `calc:iimport` Imports electronic couplings from xml of xtp-dipro using folders of pairdump

option	default	unit	description
idft_jobs_file			idft jobs file
probabilityfile_h	ianalyze.ispatial.h.out		For coarse grained simulations provide here the distance dependent means and sigmas of hole transfer integrals. This file can be created using the <code>ianalyze</code> calculator.
probabilityfile_e	ianalyze.ispatial.e.out		For coarse grained simulations provide here the distance dependent means and sigmas of electron transfer integrals. This file can be created using the <code>ianalyze</code> calculator.

1595 Return to the description of `iimport`.

1596 **4.2.19 izindo**

1597 `calc:izindo` Semiempirical electronic coupling elements for all neighbor list pairs

option	default	unit	description
orbitalsXML			File with paths to .orb files

1598 Return to the description of `izindo`.

1599 **4.2.20 jobwriter**

1600 `calc:jobwriter` Writes list of jobs for a parallel execution

option	default	unit	description
keys			job type
single_id			Segment ID as argument for <code>mps.single</code>
kmc_cutoff		nm	Pair-interaction cut-off as argument for <code>mps.kmc</code>

1601 Return to the description of `jobwriter`.

1602 **4.2.21 pairdump**

1603 `calc:pairdump` Coordinates of molecules and pairs from the neighbor list

option	default	unit	description
molecules			If <code>**true**</code> outputs single molecules, otherwise only pairs

1604 Return to the description of `pairdump`.

1605 4.2.22 `panalyze`

1606 `calc:panalyze`

Probability of neighbours being in the pair list as a function of their centre of mass distance

option	default	unit	description
resolution_space		nm	Spatial resolution for the probability function.

1607 Return to the description of `panalyze`.

1608 4.2.23 `profile`

1609 `calc:profile`

Density and site energy profiles

option	default	unit	description
axis			Axis along which to calculate density and energy profiles
direction	0 0 1		Axis direction
min		nm	Minimal projected position for manual binning
max		nm	Maximal projected position for manual binning
bin	0.1	nm	Spatial resolution of the profile
auto	1		'0' for manual binning using min and max, '1' for automated
particles			
type	segments		What centers of mass to use: 'segments' or 'atoms'
first	1		ID of the first segment
last	-1		ID of the last segment, -1 is the list end
output			
density	density.dat		Density profile file
energy	energy.dat		Energy profile file

1610 Return to the description of `profile`.

1611 4.2.24 `rates`

1612 `calc:rates`

Hopping rates using classical or semi-classical expression

option	default	unit	description
field			Field in x y z direction
temperature		K	Temperature for rates
method			Method chosen to compute rates. Can either be <code>**marcus**</code> or <code>**jortner**</code> . The first is the high temperature limit of Marcus theory, the second is the rate proposed by Jortner and Bixon
nmaxvib	20		If the method of choice is <code>**jortner**</code> , the maximal number of excited vibrations on the molecules has to be specified as an integer for the summation
omegavib	0.2	eV	If the method of choice is <code>**jortner**</code> , the vibration frequency of the quantum mode has to be given in units of eV. The default value is close to the CC bond-stretch at 0.2eV

1613 Return to the description of `rates`.

1614 4.2.25 `sandbox`

1615 `calc:sandbox`

Sandbox to test xtp classes

option	default	unit	description
--------	---------	------	-------------

ID			Not in use
----	--	--	------------

1616 Return to the description of `sandbox`.

1617 **4.2.26 stateserver**

calc:stateserver

1618 Export SQLite file to human readable format

option	default	unit	description
out			Output file name
pdb			PDB coordinate file name
keys			Sections to write to readable format (topology, segments, pairs, coordinates)

1619 Return to the description of `stateserver`.

1620 **4.2.27 tdump**

calc:tdump

1621 Coarse-grained and back-mapped (using rigid fragments) trajectories

option	default	unit	description
md	MD.pdb		Name of the coarse-grained trajectory
qm	QM.pdb		Name of the trajectory with back-substituted rigid fragments
frames	1		Number of frames to output

1622 Return to the description of `tdump`.

1623 **4.2.28 vaverage**

calc:vaverage

1624 Computes site-centered velocity averages from site occupancies

option	default	unit	description
carriers			Carrier types for which to compute velocity averages
tabulate			Tabulate 'atoms' or 'segments'

1625 Return to the description of `vaverage`.

1626 **4.2.29 zmultipole**

calc:zmultipole

1627 Evaluates polarization contribution based on the Thole model

option	default	unit	description
multipoles			Polar Site Definitions in GDMA punch-file format
control			Control options for induction computation
induce	1		Enter '1' / '0' to toggle induction on / off
first			First segment for which to compute site energies
last			Last segment for which to compute site energies
output			File to write site energies to. Site energies are also stored in the state file
check			Check mapping of polar sites to fragment
tholeparam			Thole parameters required for charge-smearing
cutoff		nm	Cut-off beyond which all interactions are neglected
cutoff2		nm	Cut-off beyond which polarization is neglected
expdamp			Damping exponent used in exponential damping function

scaling			1-n interaction scaling, currently not in use
esp			Control options for potential calculation
calcESP			Enter '1' / '0' to toggle on / off. If '1', site energies will not be evaluated
cube			
grid			XYZ file specifying grid points for potential evaluation
output			File to write grid-point potential to
esf			Control options for field calculation
calcESF			Enter '1' / '0' to toggle on / off. If '1', site energies will not be evaluated
grid			XYZ file specifying grid points for field evaluation
output			File to write grid-point field to
alphamol			Control options for molecular-polarizability calculation
calcAlpha			Enter '1' / '0' to toggle on / off. If '1', site energies will not be evaluated
output			File to write polarizability tensor in global frame and in diagonal form to
convparam			Convergence parameters for self-consistent field calculation
wSOR_N			Mixing factor for successive overrelaxation of neutral system, usually between 0.3 and 0.5
wSOR_C			Mixing factor for successive overrelaxation of charged system, usually between 0.3 and 0.5
tolerance			Convergence criterion, fulfilled if relative change smaller than tolerance
maxiter			Maximum number of iterations in the convergence loop

1628 [Return to the description of `zmultipole`.](#)

1629 **4.2.30 edft**

calc:edft

1630 A wrapper for first principles based single site calculations

option	default	unit	description
tasks	input,run,parse		What to run
store	orbitals		What to store

1631 [Return to the description of `edft`.](#)

1632 **4.2.31 idft**

calc:idft

1633 Projection method for electronic couplings. Requires edft output

option	default	unit	description
tasks	input,run,parse		What to do
store	orbitals,overlap		What to store
degeneracy	0	eV	Criterion for the degeneracy of two levels
levels	3		Output between HOMO, ..., HOMO-levels; LUMO, ..., LUMO+levels
trim	2		Use trim*occupied of virtual orbitals

1634 [Return to the description of `idft`.](#)

1635 **4.2.32 qmmm**

calc:qmmm

1636 QM/MM with the Thole MM model

option	default	unit	description
pdb_check			PDB file of polar sites
write_chk	dipoles.xyz		XYZ file with dipoles split onto point charges
format_chk	xyz		format, gaussian or xyz
split_dpl	1		'0' do not split dipoles onto point charges, '1' do split
dpl_spacing	1e-3	nm	Spacing to be used when splitting dipole onto point charges: $d = q * a$
dftpackage			DFT package to use for the QM region
gwbse			Specify if GW/BSE excited state calculation ist needed
gwbse_options			GW/BSE options file
state			Number of excited state, which is to be calculated
type			Character of the excited state to be calculated
filter			Filter with which to find the excited state after each calculation
oscillator_strength			Oscillator strength filter, only states with higher oscillator strength are considered
charge_transfer			Charge transfer filter , only states with charge transfer above threshold are considered
qmmmconvg			convergence criteria for the QM/MM
dR	0.001	nm	RMS of coordinates
dQ	0.001	e	RMS of charges
dE_QM	0.0001	eV	Energy change of the QM region
dE_MM	0.0001	eV	Energy change of the MM region
max_iter	10		Number of iterations
coulombmethod			Options for the MM embedding
method	cut-off		Method for evaluation of electrostatics
cutoff1			Cut-off for the polarizable MM1 shell
cutoff2			Cut-off for the static MM2 shell
tholemodel			Parameters for teh Thole model
induce			'1' - induce '0' - no induction
induce_intra_pair			'1' - include mutual interaction of induced dipoles in the QM region. '0' - do not
exp_damp	0.39		Sharpness parameter
scaling			Bond scaling factors
convergence			Convergence parameters for the MM1 (polarizable) region
wSOR_N			Mixing factor for the successive overrelaxation algorithm for a neutral QM region
wSOR_C			Mixing factor for the successive overrelaxation algorithm for a charged QM region
max_iter	512		Maximal number of iterations to converge induced dipoles
tolerance			Maximum RMS change allowed in induced dipoles

1637 Return to the description of qmmm.

1638 4.2.33 xqmultipole

calc:xqmultipole
1639

Electrostatic interaction and induction energy of charged molecular clusters

option	default	unit	description
mapping			Polar-site mapping definition
job_file			Job file
emp_file			Polar-background definition, allocation of mps-files to segments
pdb_check			Whether or not to output a pdb-file of the mapped polar sites
format_chk			Format for check-file: 'xyz' or 'gaussian'

split_dpl			Split dipoles onto point charges in check-file
dpl_spacing		nm	Spacing between point charges for check-file output
coulombmethod			
method			Currently only cut-off supported
cutoff1		nm	Full-interaction radius cut-off
cutoff2		nm	Radius of electrostatic buffer
tholemodel			
induce			Induce - or not
induce_intra_pair			Induce mutually within the charged cluster
exp_damp			Thole sharpness parameter
scaling			Bond scaling parameters, currently not used
convergence			
wSOR_N			SOR mixing factor for overall neutral clusters
wSOR_C			SOR mixing factor for overall charged clusters
max_iter			Maximum number of iterations
tolerance			Relative tolerance as convergence criterion

1640 Return to the description of `xqmultipole`.

1641 4.2.34 `energy2xml`

`calc:energy2xml`

1642 Write out energies from SQL file

option	default	unit	description
--------	---------	------	-------------

1643 Return to the description of `energy2xml`.

1644 4.2.35 `integrals2xml`

`calc:integrals2xml`

1645 Write out transfer integrals from SQL file

option	default	unit	description
--------	---------	------	-------------

1646 Return to the description of `integrals2xml`.

1647 4.2.36 `occupations2xml`

`calc:occupations2xml`

1648 Write out site occupation probabilities from SQL file

option	default	unit	description
--------	---------	------	-------------

1649 Return to the description of `occupations2xml`.

1650 4.2.37 `pairs2xml`

`calc:pairs2xml`

1651 Write out neighbourlist from SQL file

option	default	unit	description
--------	---------	------	-------------

1652 Return to the description of `pairs2xml`.

1653 4.2.38 `rates2xml`

`calc:rates2xml`

1654 Write out charge transfer rates from SQL file

option	default	unit	description
--------	---------	------	-------------

1655 Return to the description of `rates2xml`.

1656 **4.2.39 segments2xml**

`calc.segments2xml`

1657 Write out segment data from SQL file

option	default	unit	description
--------	---------	------	-------------

1658 Return to the description of `segments2xml`.

1659 **4.2.40 trajectory2pdb**

`calc.trajectory2pdb`

1660 Generate PDB files for the mapped MD/QM topology

option	default	unit	description
--------	---------	------	-------------

1661 Return to the description of `trajectory2pdb`.

1662 **4.3 Common options**

`ref.options`

name	Description of the option
------	---------------------------

Bibliography

- ruhle_microscopic_2011 [1] V. RÅijhle *et al.*, J. Chem. Theory Comput. **7**, 3335 (2011), bibtex: ruhle_microscopic_2011. [ii](#), [3](#), [19](#)
- ruhle_versatile_2009 [2] V. RÅijhle *et al.*, J. Chem. Theory Comput. **5**, 3211 (2009), bibtex: ruhle_versatile_2009. [ii](#), [3](#), [6](#)
- gamma_design_1995 [3] E. Gamma, R. Helm, and R. E. Johnson, *Design Patterns. Elements of Reusable Object-Oriented Software.*, 1st ed., reprint. ed. (Addison-Wesley Longman, Amsterdam, ADDRESS, 1995), bibtex: gamma_design_1995. [3](#)
- ruhle_multiscale_2010 [4] V. RÅijhle, J. Kirkpatrick, and D. Andrienko, J. Chem. Phys. **132**, 134103 (2010), bibtex: ruhle_multiscale_2010. [7](#)
- vukmirovic_charge_2008 [5] N. VukmiroviÄŒ and L.-W. Wang, J. Chem. Phys. **128**, 121102 (2008), bibtex: vukmirovic_charge_2008. [7](#)
- vukmirovic_charge_2009 [6] N. VukmiroviÄŒ and L.-W. Wang, Nano Letters **9**, 3996 (2009), bibtex: vukmirovic_charge_2009.
- mcmahon_ad_2009 [7] D. P. McMahon and A. Troisi, Chem. Phys. Lett. **480**, 210 (2009), bibtex: mcmahon_ad_2009. [7](#)
- bredas_charge-transfer_2004 [8] J.-L. BrÅÍdas, D. Beljonne, V. Coropceanu, and J. Cornil, Chem. Rev. **104**, 4971 (2004), bibtex: bredas_charge-transfer_2004. [9](#), [19](#)
- may_relationship_2011 [9] F. May *et al.*, J. Mater. Chem. **21**, 9538 (2011), bibtex: may_relationship_2011. [9](#), [20](#)
- breneman_determining_1990 [10] C. M. Breneman and K. B. Wiberg, J. Comput. Chem. **11**, 361 (1990), bibtex: breneman_determining_1990. [11](#)
- stone_distributed_1985 [11] A. Stone and M. Alderton, Molecular Physics **56**, 1047 (1985), bibtex: stone_distributed_1985. [11](#), [12](#)
- chirlian_atomic_1987 [12] L. E. Chirlian and M. M. Francl, J. Comput. Chem. **8**, 894 (1987), bibtex: chirlian_atomic_1987. [11](#)
- singh_approach_1984 [13] U. C. Singh and P. A. Kollman, J. Comput. Chem. **5**, 129 (1984), bibtex: singh_approach_1984. [11](#)
- stone_distributed_2005 [14] A. J. Stone, J. Chem. Theory Comput. **1**, 1128 (2005), bibtex: stone_distributed_2005. [11](#), [12](#)
- stone_theory_1997 [15] A. J. Stone, *The Theory of intermolecular forces* (Clarendon Press, Oxford, 1997), bibtex: stone_theory_1997. [12](#)
- thole_molecular_1981 [16] B. Thole, Chem. Phys. **59**, 341 (1981), bibtex: thole_molecular_1981. [13](#)
- van_duijnen_molecular_1998 [17] P. T. van Duijnen and M. Swart, J. Phys. Chem. A **102**, 2399 (1998), bibtex: van_duijnen_molecular_1998-1. [13](#)
- applequist_atom_1972 [18] J. Applequist, J. R. Carl, and K.-K. Fung, J. Am. Chem. Soc. **94**, 2952 (1972), bibtex: applequist_atom_1972. [13](#)
- ren_polarizable_2003 [19] P. Ren and J. W. Ponder, J. Phys. Chem. B **107**, 5933 (2003), bibtex: ren_polarizable_2003. [13](#)
- baessler_charge_1993 [20] H. Baessler, Phys. Status Solidi B **175**, 15 (1993), bibtex: baessler_charge_1993. [14](#), [19](#)
- troisi_charge-transport_2006 [21] A. Troisi and G. Orlandi, Phys. Rev. Lett. **96**, (2006), bibtex: troisi_charge-transport_2006.
- troisi_charge_2009 [22] A. Troisi, D. L. Cheung, and D. Andrienko, Phys. Rev. Lett. **102**, 116602 (2009), bibtex: troisi_charge_2009.
- mcmahon_organic_2010 [23] D. P. McMahon and A. Troisi, ChemPhysChem **11**, 2067 (2010), bibtex: mcmahon_organic_2010.
- vehoff_charge_2010 [24] T. Vehoff *et al.*, J. Phys. Chem. C **114**, 10592 (2010), bibtex: vehoff_charge_2010. [14](#)
- baumeier_density-functional_2010 [25] B. Baumeier, J. Kirkpatrick, and D. Andrienko, Phys. Chem. Chem. Phys. **12**, 11103 (2010), bibtex: baumeier_density-functional_2010. [14](#), [17](#), [19](#)
- kirkpatrick_approximate_2008 [26] J. Kirkpatrick, Int. J. Quantum Chem. **108**, 51 (2008), bibtex: kirkpatrick_approximate_2008. [18](#)
- walker_electrical_2002 [27] A. B. Walker, A. Kambili, and S. J. Martin, J. Phys-Condens. Mat. **14**, 9825 (2002), bibtex: walker_electrical_2002. [19](#)

- [borsenberger_charge_1991](#) [28] P. M. Borsenberger, L. Pautmeier, and H. BÄd’ssler, *J. Chem. Phys.* **94**, 5447 (1991), bibtex: borsenberger_charge_1991.
- [pasveer_unified_2005](#) [29] W. F. Pasveer *et al.*, *Phys. Rev. Lett.* **94**, 206601 (2005), bibtex: pasveer_unified_2005. [19](#)
- [bredas_molecular_2009](#) [30] J.-L. BrÄydas, J. E. Norton, J. Cornil, and V. Coropceanu, *Accounts Chem. Res.* **42**, 1691 (2009), bibtex: bredas_molecular_2009. [19](#)
- [coropceanu_charge_2007](#) [31] V. Coropceanu *et al.*, *Chem. Rev.* **107**, 926 (2007), bibtex: coropceanu_charge_2007.
- [nelson_modeling_2009](#) [32] J. Nelson, J. J. Kwiatkowski, J. Kirkpatrick, and J. M. Frost, *Accounts Chem. Res.* **42**, 1768 (2009), bibtex: nelson_modeling_2009. [19](#)
- [marcus_electron_1993](#) [33] R. A. Marcus, *Rev. Mod. Phys.* **65**, 599 (1993), bibtex: marcus_electron_1993. [19](#)
- [hutchison_hopping_2005](#) [34] G. R. Hutchison, M. A. Ratner, and T. J. Marks, *J. Am. Chem. Soc.* **127**, 2339 (2005), bibtex: hutchison_hopping_2005. [19](#)
- [chang_new_2005](#) [35] J.-L. Chang, *J. Mol. Spectrosc.* **232**, 102 (2005), bibtex: chang_new_2005. [20](#)
- [hoffman_reorganization_1996](#) [36] B. M. Hoffman and M. A. Ratner, *Inorg. Chim. Acta.* **243**, 233 (1996), bibtex: hoffman_reorganization_1996. [20](#)
- [bortz_new_1975](#) [37] A. B. Bortz, M. H. Kalos, and J. L. Lebowitz, *J. Comput. Phys.* **17**, 10 (1975), bibtex: bortz_new_1975. [21](#)
- [scher_anomalous_1975](#) [38] H. Scher and E. Montroll, *Phys. Rev. B* **12**, 2455 (1975), bibtex: scher_anomalous_1975. [21](#)
- [borsenberger_role_1993](#) [39] P. M. Borsenberger, E. H. Magin, M. D. VanAuweraer, and F. C. D. Schryver, *Phys. Status Solidi A* **140**, 9 (1993), bibtex: borsenberger_role_1993. [21](#)
- [derrida_velocity_1983](#) [40] B. Derrida, *J. Stat. Phys.* **31**, 433 (1983), bibtex: derrida_velocity_1983. [21](#), [31](#)
- [cordes_one-dimensional_2001](#) [41] H. Cordes *et al.*, *Phys. Rev. B* **63**, 094201 (2001), bibtex: cordes_one-dimensional_2001.
- [seki_electric_2001](#) [42] K. Seki and M. Tachiya, *Phys. Rev. B* **65**, 014305 (2001), bibtex: seki_electric_2001. [21](#)
- [lukyanov_extracting_2010](#) [43] A. Lukyanov and D. Andrienko, *Phys. Rev. B* **82**, 193202 (2010), bibtex: lukyanov_extracting_2010. [21](#)
- [van_der_holst_modeling_2009](#) [44] J. J. M. van der Holst *et al.*, *Phys. Rev. B* **79**, 085203 (2009), bibtex: van_der_holst_modeling_2009. [30](#)
- [dunlap_charge-dipole_1996](#) [45] D. Dunlap, P. Parris, and V. Kenkre, *Phys. Rev. Lett.* **77**, 542 (1996), bibtex: dunlap_charge-dipole_1996. [31](#)
- [novikov_essential_1998](#) [46] S. V. Novikov *et al.*, *Phys. Rev. Lett.* **81**, 4472 (1998), bibtex: novikov_essential_1998. [31](#)
- [nagata_atomistic_2008](#) [47] Y. Nagata and C. Lennartz, *J. Chem. Phys.* **129**, 034709 (2008), bibtex: nagata_atomistic_2008. [31](#)
- [novikov_cluster_1995](#) [48] S. V. Novikov and A. V. Vannikov, *J. Phys. Chem.* **99**, 14573 (1995), bibtex: novikov_cluster_1995. [31](#)